AD-A083 616 HUGHES RESEARCH LABS MALIBU CA F/G 20/1
FIBER OPTIC DELAY LINE (250 KHZ - 250 MHZ).(U)
MAR 80 C W SLAYMAN, H W YEN, W H WALLACE N00173-79-C-0098
UNCLASSIFIED NL

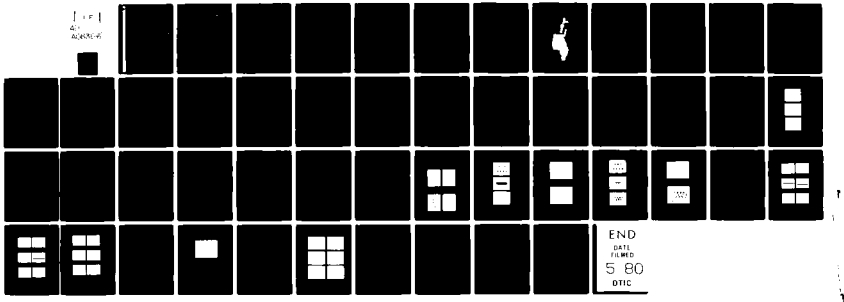

FIBER OPTIC DELAY LINE (250 kHz – 250 MHz)

C.W. Slayman, H.W. Yen, W.H. Wallace, and R.R. Burns

Hughes Research Laboratories
3011 Malibu Canyon Road
Malibu, CA 90265

March 1980

N00173–79–C–0098
Final Report
15 March 1979 through 15 September 1979

Approved for public release; distribution unlimited.

Sponsored by

NAVAL RESEARCH LABORATORY
Washington, D.C. 20375

UNCLASSIFIED

SECURITY CLASSIFICATION OF THIS PAGE (When Data Entered)

REPORT DOCUMENTATION PAGE

READ INSTRUCTIONS BEFORE COMPLETING FORM

1. REPORT NUMBER

2. GOVT ACCESSION NO.

3. RECIPIENT'S CATALOG NUMBER

4. TITLE (and Subtitle)

FIBER OPTIC DELAY LINE (250 kHz - 250 MHz).

5. TYPE OF REPORT & PERIOD COVERED

Final Report.
15 Mar [redacted]-15 Sep [redacted]79

6. PERFORMING ORG. REPORT NUMBER

7. AUTHOR(s)

C.W. Slayman, H.W. Yen, W.H. Wallace [redacted]
R.R. Burns

8. CONTRACT OR GRANT NUMBER(s)

N00173-79-C-0098

9. PERFORMING ORGANIZATION NAME AND ADDRESS

Hughes Research Laboratories
3011 Malibu Canyon Road
Malibu, CA 90265

10. PROGRAM ELEMENT, PROJECT, TASK AREA & WORK UNIT NUMBERS

12) 50

11. CONTROLLING OFFICE NAME AND ADDRESS

Naval Research Laboratory
4555 Overlook Ave., S.W.
Washington, DC 20375

12. REPORT DATE

Mar [redacted]80

13. NUMBER OF PAGES

50

14. MONITORING AGENCY NAME & ADDRESS(if different from Controlling Office)

15. SECURITY CLASS. (of this report)

UNCLASSIFIED

15a. DECLASSIFICATION DOWNGRADING SCHEDULE

16. DISTRIBUTION STATEMENT (of this Report)

Approved for public release; distribution unlimited

17. DISTRIBUTION STATEMENT (of the abstract entered in Block 20, if different from Report)

18. SUPPLEMENTARY NOTES

19. KEY WORDS (Continue on reverse side if necessary and identify by block number)

Delay line, Optical fiber, GaAlAs injection laser, PIN photodiode

20. ABSTRACT (Continue on reverse side if necessary and identify by block number)

Three stabilized semiconductor laser transmitters, one photodiode-amplifier module, and one 475-m section of optical fiber were packaged for application in a fiber-optic delay line. The design and performance of the transmitter and receiver are presented over a bandwidth of 50 kHz to 350 MHz. The entire system, consisting of a transmitter-fiber-receiver, displays a dynamic range of 30 dB or better and a pulse delay of 2.2 μsec. The system is flat to ±1 dB across the entire band.

DD FORM 1 JAN 73 1473 EDITION OF 1 NOV 65 IS OBSOLETE

UNCLASSIFIED

SECURITY CLASSIFICATION OF THIS PAGE (When Data Entered)

172,600

TABLE OF CONTENTS

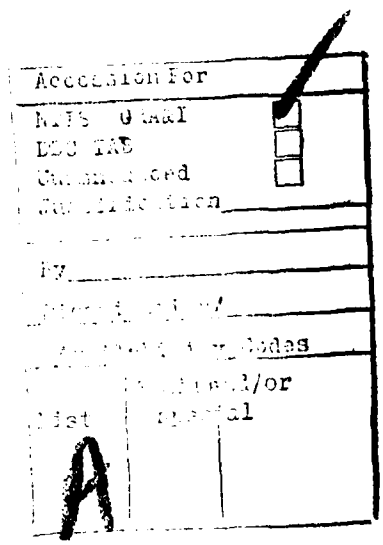

LIST OF ILLUSTRATIONS

SECTION 1

INTRODUCTION

This report describes the design and performance of the 250 kHz to 250 MHz fiber-optic delay line. Three diode laser transmitters, one 475-m length of multimode graded-index fiber, and one photodiode-amplifier module were suitably packaged for delivery to NRL. The performance specifications of the delay line are as follows:

- Bandwidth — 250 kHz to 250 MHz was the original specification. However, NRL later expressed a desire for a cut-off below 250 kHz.
- Throughput Flatness — ±1 dB across the band
- Linearity — Second harmonic 45 dB below the fundamental. NRL later suggested that a 1 dB compression level would be more meaningful.
- Dynamic Range — 30 dB (or greater)
- Amplitude Stabilization — ±0.1%. This specification has no effect on the performance of the delay line.

Table 1 summarizes the performance obtained from the three laser transmitters used in conjunction with the fiber and receiver. Figure 1 is a photograph of the three transmitters, the fiber and connectors, and the photodiode-amplifier receiver.

Table 1. Summary of the Characteristics of the Fiber-Optic Delay Line

Quantity	Tx 1	Tx 2	Tx 3
±1 dB bandwidth	50 kHz to 500 MHz	50 kHz to 300 MHz	30 kHz to 300 MHz
Throughput gain, dB	0	5.6	6.6
1 dB input compression power, dBm	>-5	>0	>-10
Equivalent noise at input, dBm	-35±3	-36±3	-39±2
Dynamic range, dB	>30±3	>36±3	>29±3
CW output at pigtail, μW	389	783	378
CW fluctuation, %	<±0.3	<±0.7	<±0.3
Delay, μsec	2.2	2.2	2.2

7037

M13270

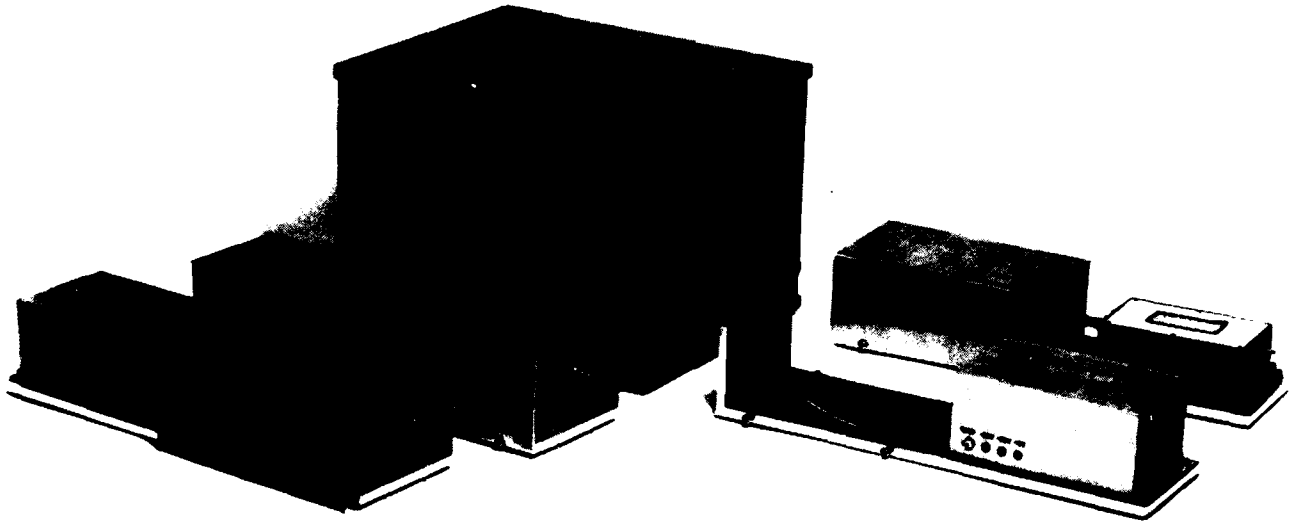

Figure 1. Laser transmitters, fiber delay, and receiver.

SECTION 2

FIBER-OPTIC DELAY LINE COMPONENTS

A. TRANSMITTER DESIGN

Three semiconductor laser transmitters were designed and built on the project. Three Hitachi Ltd. buried heterostructure lasers (Model No. HLP-2500) were selected for their low threshold current, single-mode output, and linear optical power output versus current.

Each of the three transmitters is temperature stabilized at 20°C by thermoelectric coolers. A photodiode at the monitor port of the laser is used in a feedback circuit to stabilize the cw power of the laser. Figure 2 is a schematic of the transmitter stage. Figures 3 and 4 are the thermal and optical stabilization circuits, respectively. Figure 5 is the embedding network of the laser for the stabilized dc bias current and the capacitively coupled rf input. With a forward-biased diode resistance of 13 Ω, the nominal VSWR is 1.1 to 1.

The cw output of each transmitter is given in Table 2. The long-term stability (∿10 min) of each transmitter is also shown. An EG&G 550-1 radiometer photometer was used to make the measurements.

The drive voltages for the transmitters are +15 V and -15 V for the control circuits and +3 to +5 V for the thermoelectric cooler. At normal ambient temperatures, +3 V is sufficient drive for the cooler to cycle from on to off in roughly 2-sec cycles. For high ambient temperatures, since the cooler will continuously draw current, the drive should be increased to +5 V to handle the added thermal load.

Table 2. CW Transmitter Characteristics

Transmitter	P_{cw}, μW	Fluctuation, %
Tx 1	389	<±0.3
Tx 2	783	<±0.7
Tx 3	378	<±0.3

7037

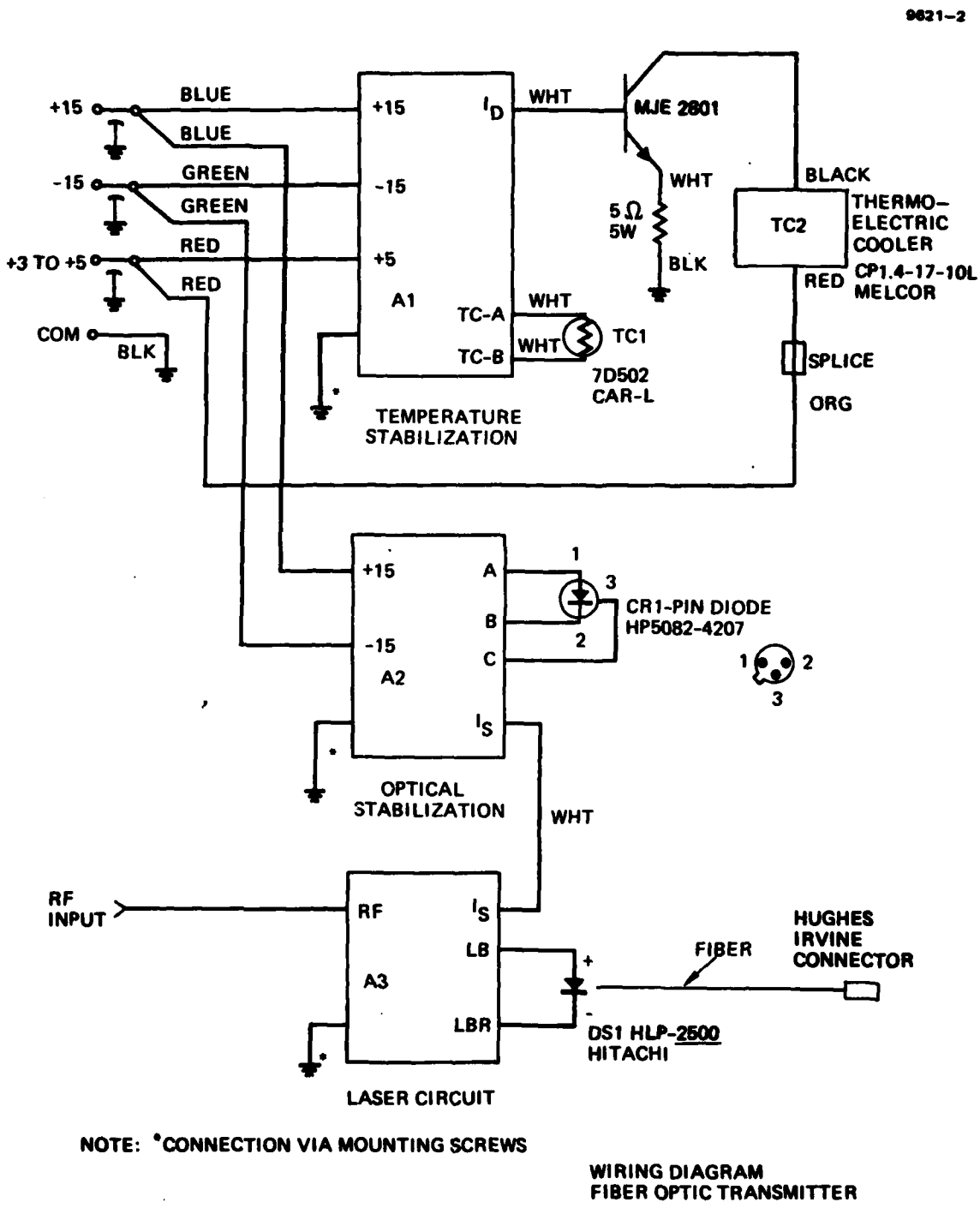

Figure 2. Transmitter circuit.

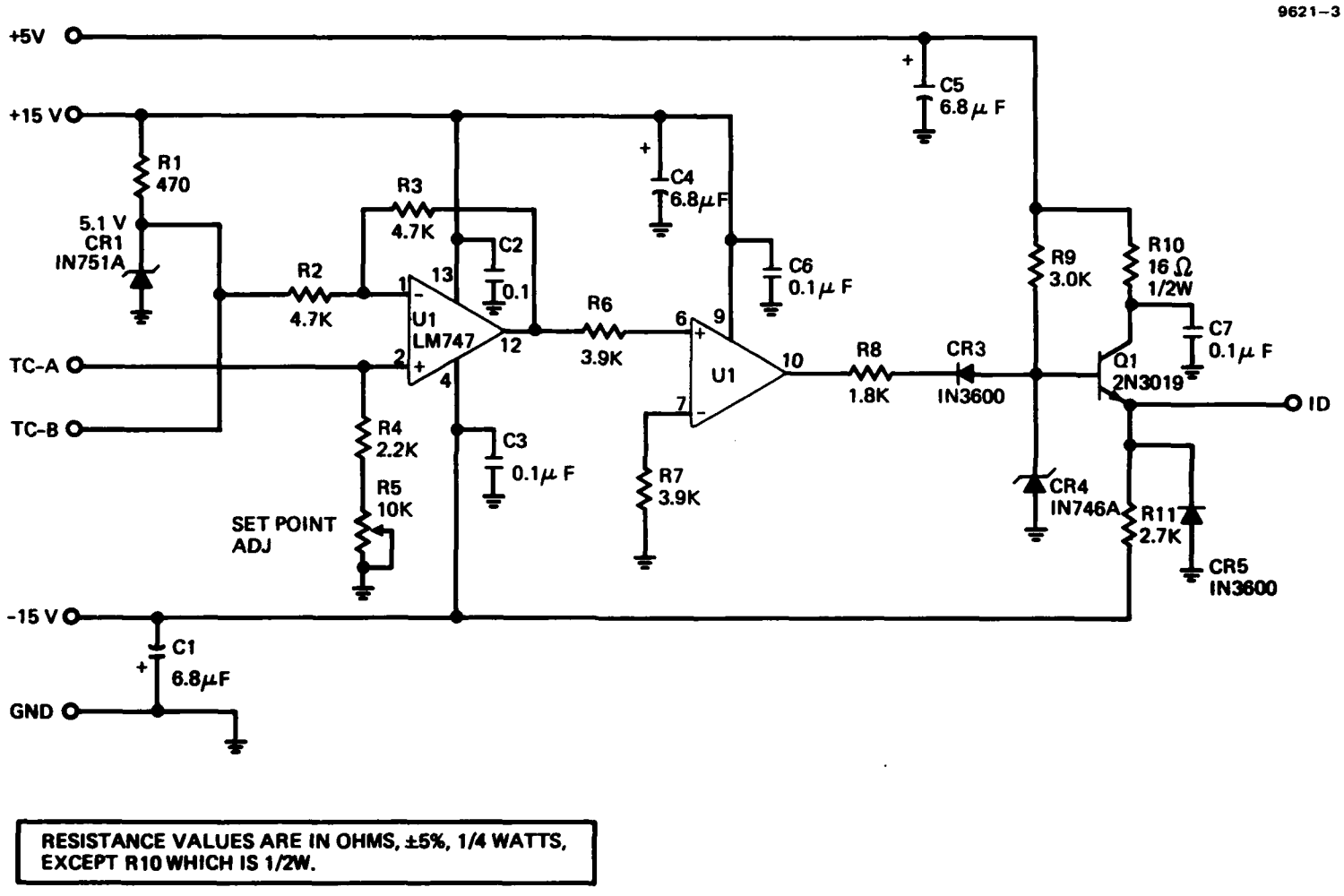

Figure 3. Temperature stabilization circuit.

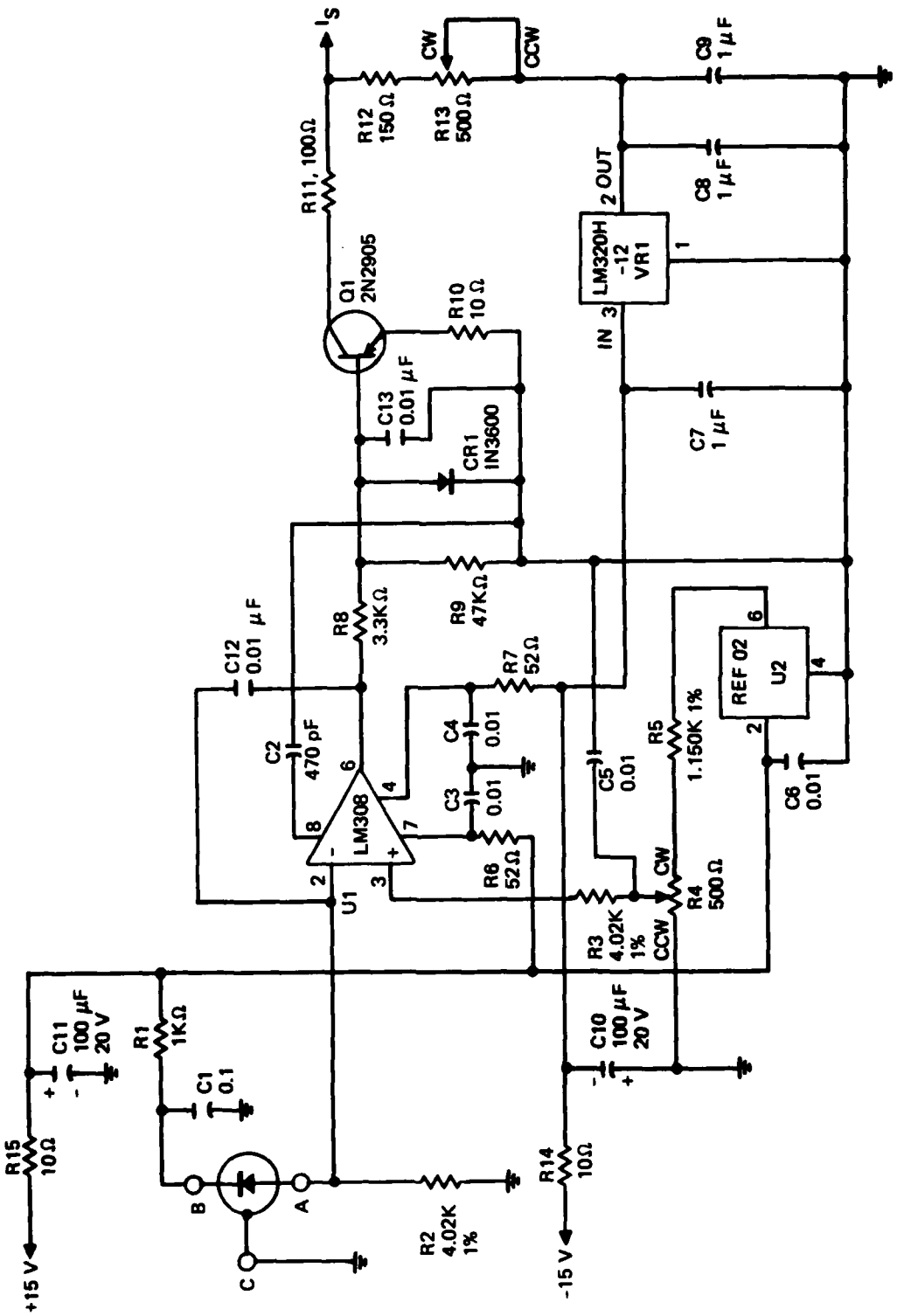

Figure 4. Optical stabilization circuit.

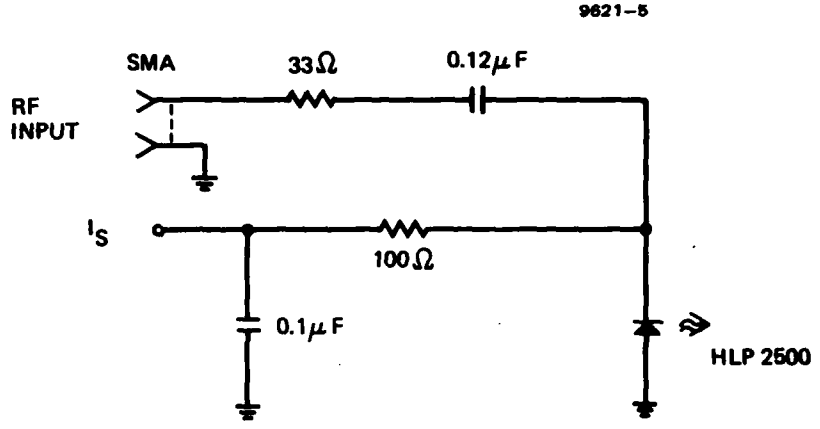

Figure 5. Laser rf and dc input circuit.

B. OPTICAL FIBER

A 475-m length of Corning 5040 graded-index fiber is used for the delay. The bandwidth of the fiber is 400 MHz·km, or 840 MHz for the 475-m section. Two Hughes (Irvine) fiber connectors have been placed on the fiber to allow it to be connected and disconnected from the transmitters and receiver.

The fiber loss was measured to be 9 dB/km (or 4.3 dB) on the optical time domain reflectometer (OTDR) at a wavelength of 900 nm. The fiber loss was determined at the 820-nm wavelength of the transmitter by measuring the power out of the transmitter connector (Table 2) and then measuring the power out of the fiber with the transmitter connected to it. Table 3 summarizes these results.

Table 3. Fiber Loss at 820 nm for the Three Transmitters

Transmitter	Fiber Loss, dB
Tx 1	3.7 to 4.8
Tx 2	3.5 to 4.3
Tx 3	3.5 to 3.6

7037

The scatter in the data is due to the reproducibility of the connector loss. The data in Table 3 represents the result of several connect-disconnect tests.

C. RECEIVER DESIGN

A PIN photodetector was chosen over an avalanche photodiode (APD) in the final receiver design for two reasons: (1) the sensitivity of the photocurrent multiplication factor M to temperature and bias voltage requires a temperature and bias-stabilized receiver, and (2) the

allowable cw optical power into an APD is less than that into a PIN photodetector because typical high-speed photodetectors are damaged at power levels near 100 mW (optical plus electronic). For example, the power from the fiber output is in excess of 100 μW for all three transmitters. With a detector responsivity (M = 1) of ∿0.3 μA/μW, the PIN photocurrent would be 30 μA, and thus the electronic power at 100 V bias would only be 3 mW. However, if the APD has a gain of M = 33 at 100 V, then the dc photocurrent would be 1 mA and the electronic power of 100 mW would cause detector damage.

Two PIN diodes were studied for use as the optical demodulator in the receiver circuit. The first was a small-area (0.5×10^{-3} cm^2) Hewlett-Packard 5082-4205 PIN. The lens was removed from the pill package, and a short section of fiber (Corning 5040) was connected and epoxied to the package. A large-area (8×10^{-3} cm^2) Hewlett-Packard 5082-4207 was the second PIN studied. A short section of Corning fiber was also fixed to the 5082-4207, but the front window prevented the fiber from being brought close to the PIN. Both detector pigtails were optimized by maximizing the detected current (due to a cw optical beam coupled into the fiber pigtail) before epoxying.

Figure 6 shows the cw optical response of the 5028-4205 pigtail at 50-V bias. The detected current versus optical power deviates from linearity at low power levels (due to detector dark current). The pigtail begins to saturate at an input of about 1 mW. Figure 7 gives the responsivity η_I(μA/μW) of the 5082-4205 pigtail, and Figure 8 gives its response versus bias voltage. At high power levels (>100 μW), the PIN sensitivity depends on the bias voltage. This is undesirable from the standpoint of receiver stability.

Figures 9 through 11 are the same plots (as Figures 6 through 8) for the 5082-4207 pigtail. The 5082-4207 has a responsivity of $\eta_I \simeq 0.22$ μA/μW, which is slightly less than the $\eta_I \simeq 0.25$ μA/μW of the 5082-4205 pigtail. However, the 5082-4207 does not saturate until 10 mW (Figure 10) and displays no bias sensitivity up to 1 mW optical power

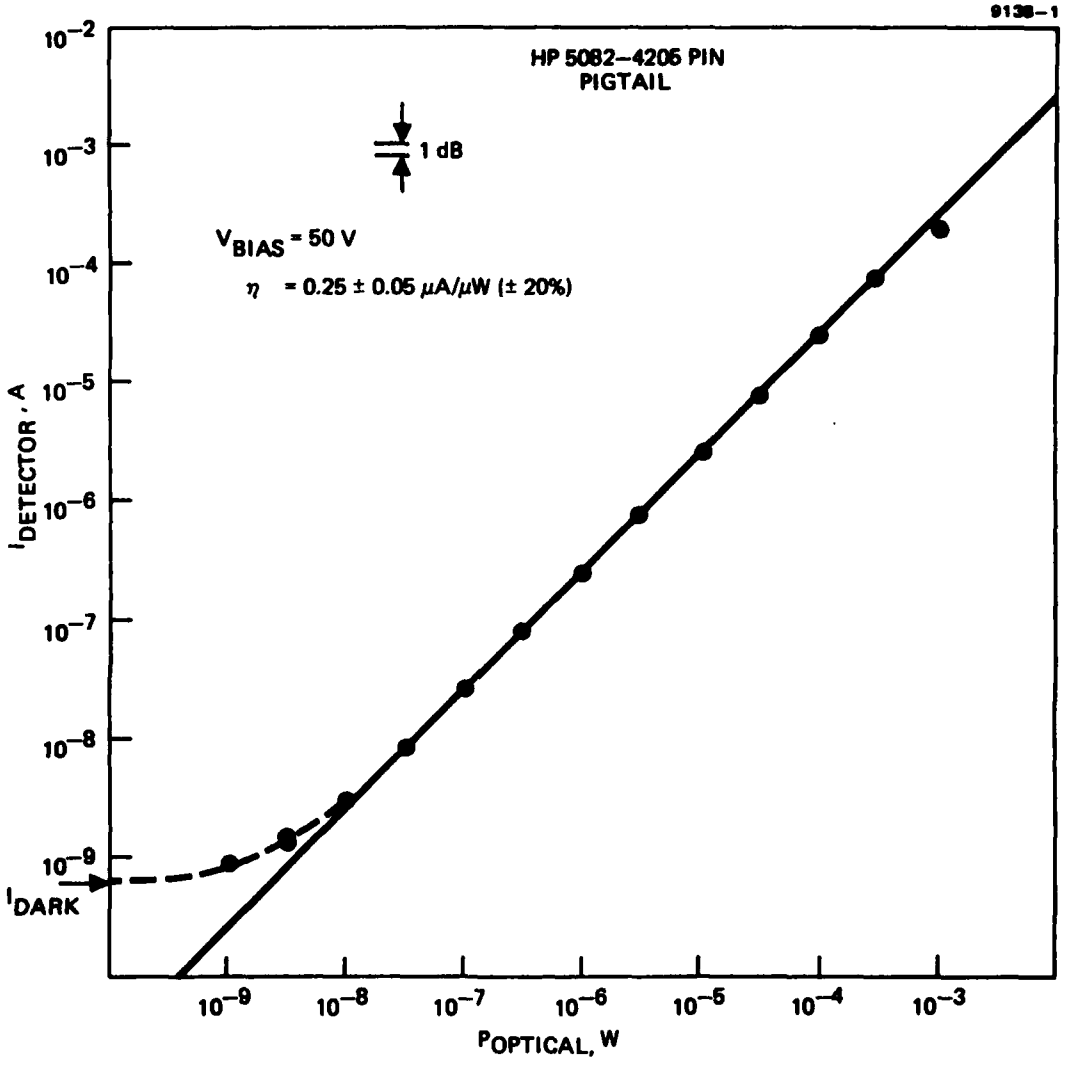

Figure 6. CW optical response of the 5082-4205 pigtail.

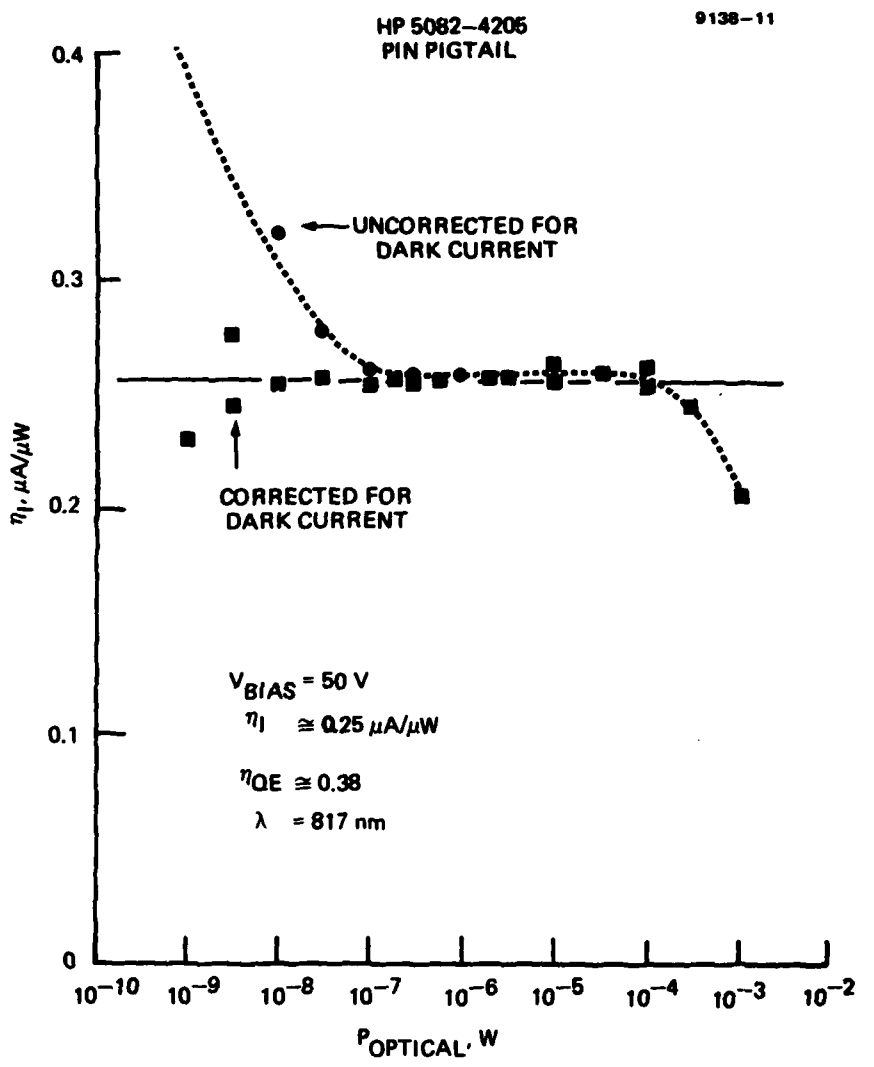

Figure 7. Responsivity η_I of the 5082-4205 pigtail.

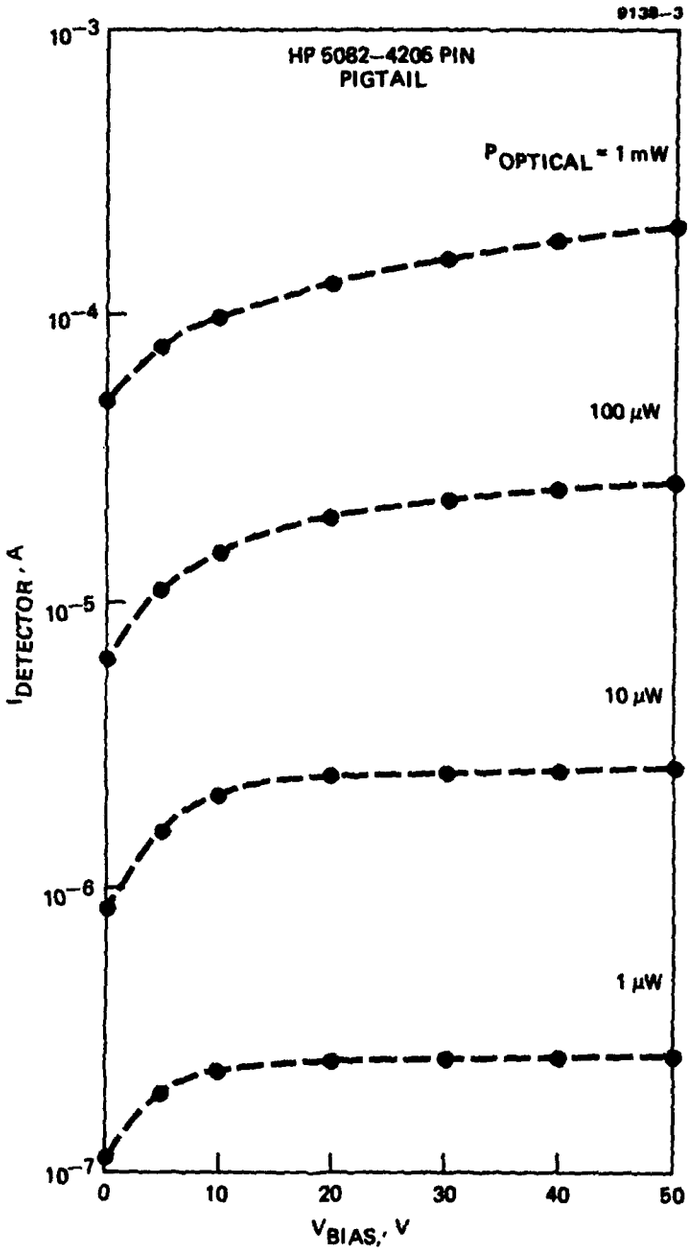

Figure 8. Detector current versus bias voltage of the 5082-4205 pigtail.

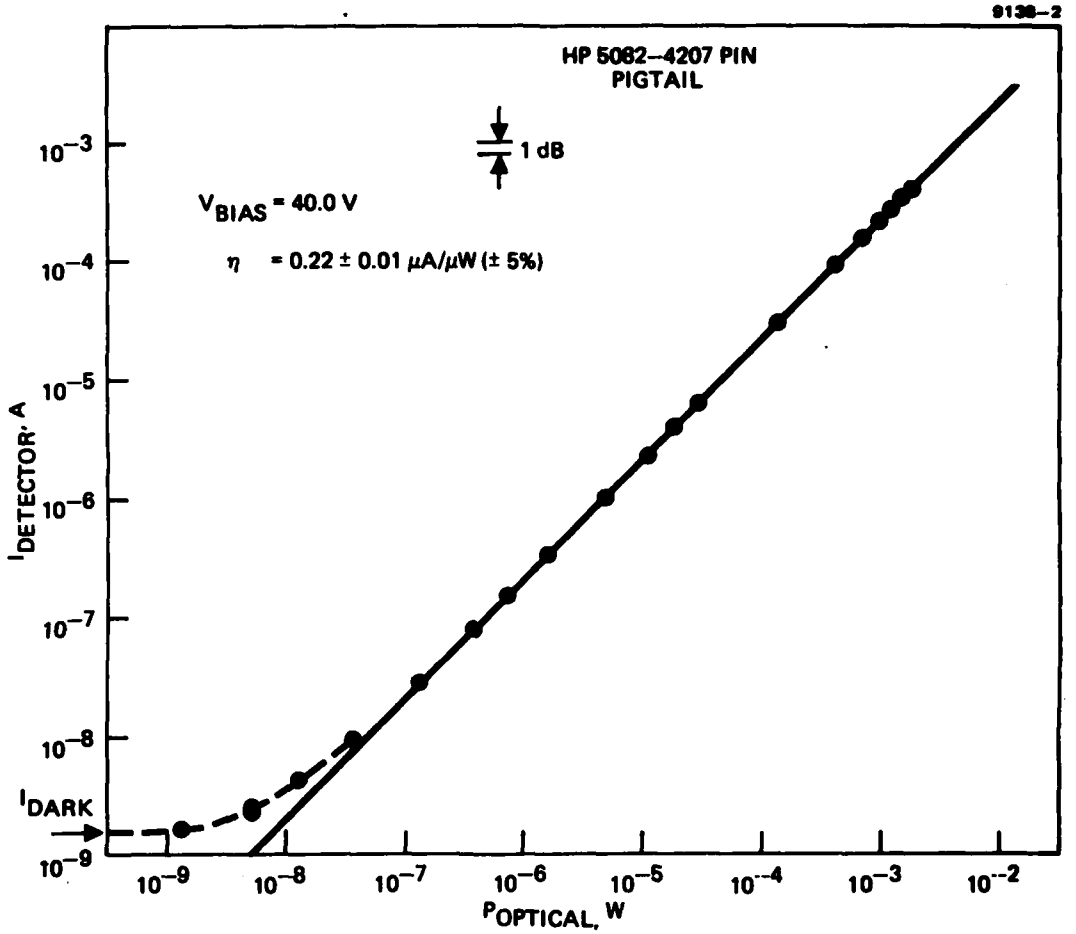

Figure 9. CW optical response of the 5082-4207 pigtail.

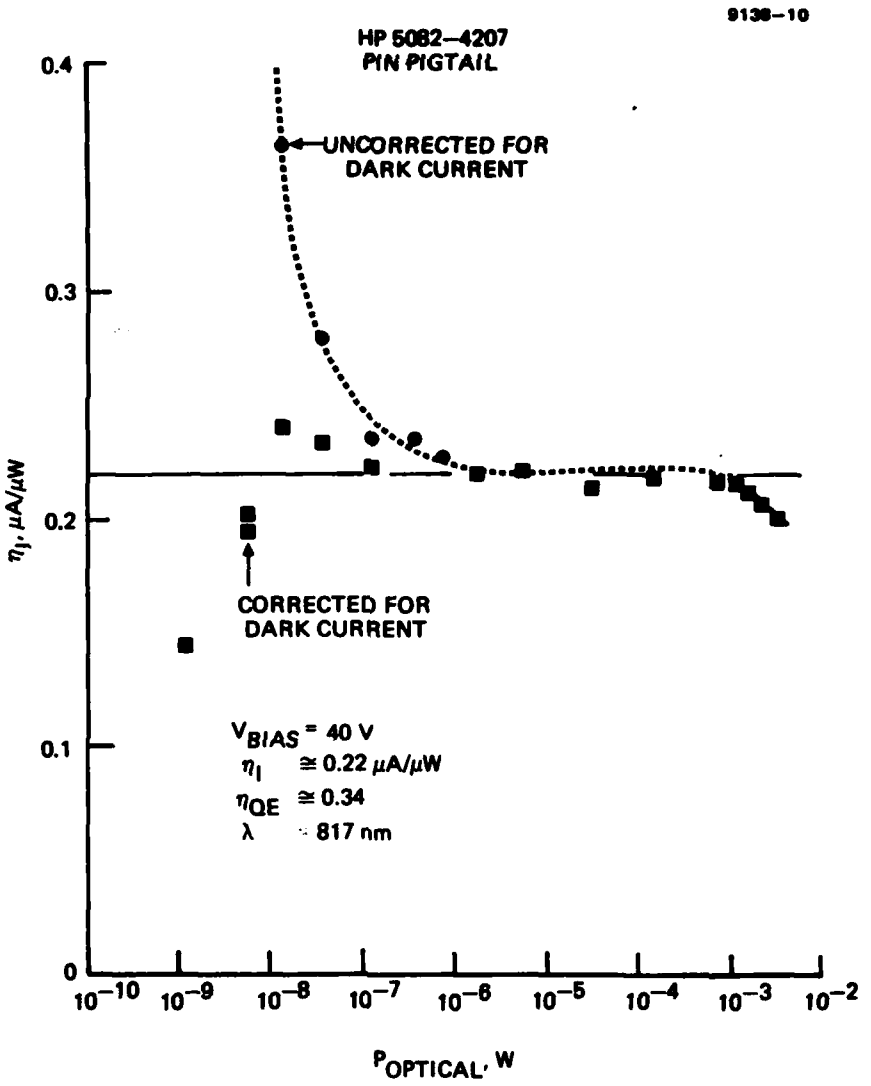

Figure 10. Responsivity of the 5082-4207 pigtail.

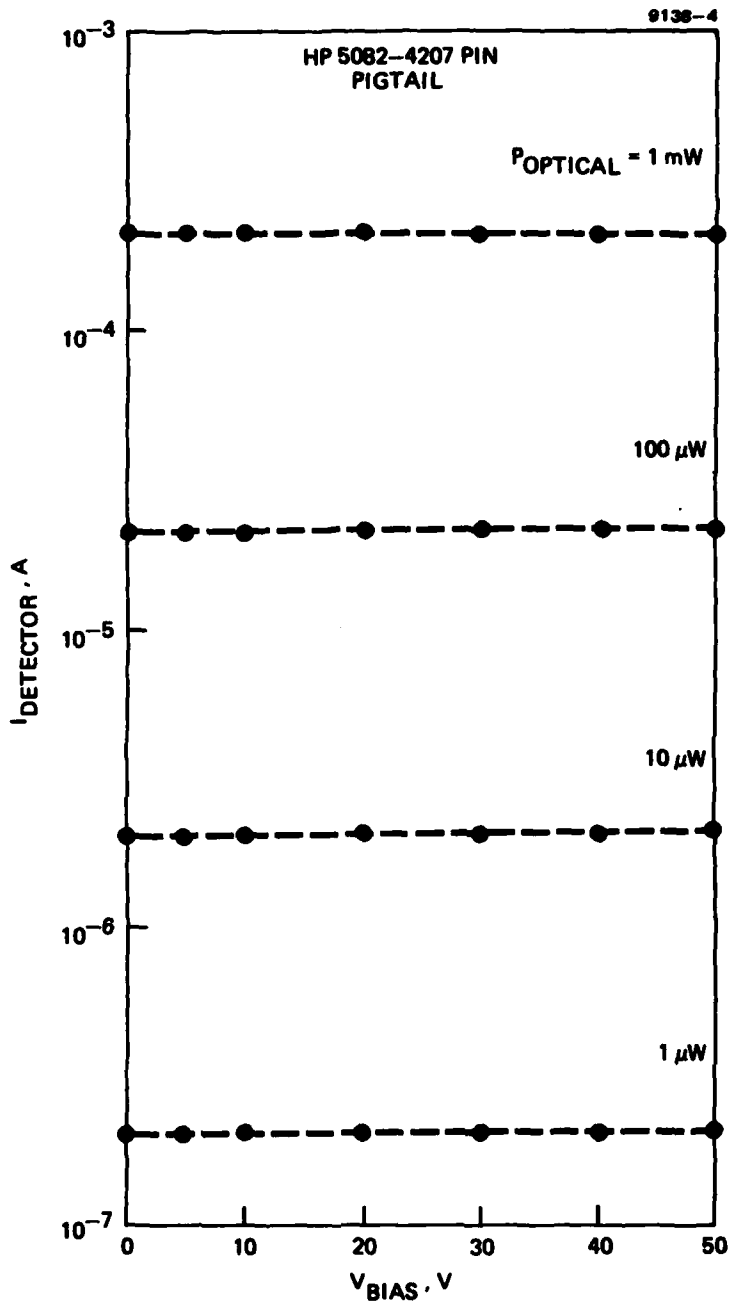

Figure 11. Detector current versus bias voltage of the 5082-4207 pigtail.

(Figure 11). These two advantages led us to select the 5082-4207 for use in the receiver.

To keep the total insertion loss of the delay line low, the photodiode was followed by a preamplifier (Avantek GPD-463) and a postamplifier (Avantek AV-1M). The circuit schematic of the receiver is shown in Figure 12. The voltages required to drive the receiver are +40 V for the photodiode, +24 V for the preamp, and +28 V for the postamp.

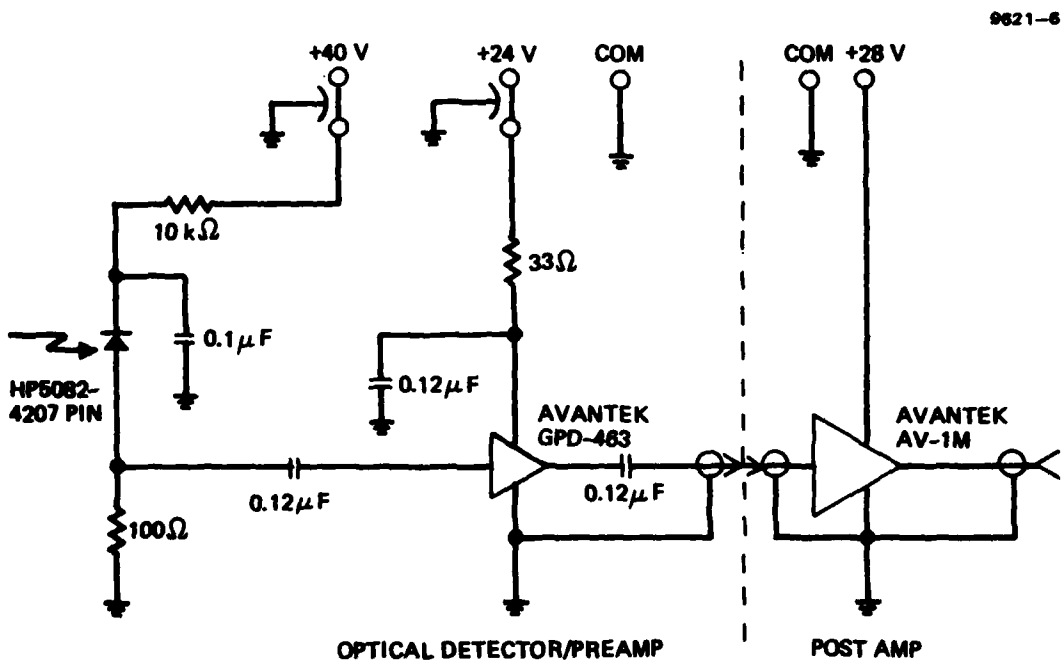

Figure 12. Fiber-optic receiver.

SECTION 3

SYSTEM PERFORMANCE

A. INSERTION LOSS OR GAIN

The microwave insertion loss of the delay line is the ratio of rf input power P_{in} to rf output power P_{out}. Due to the receiver amplifiers, the delay line actually displayed net gain for Tx 2 and Tx 3. Figure 13 is a plot of the small-signal (P_{in}<-20 dB) gain of the transmitter-fiber-receiver link versus frequency for the three transmitters. Table 4 summarizes the data presented in Figure 13. Each transmitter-delay fiber-receiver combination is flat to within ±1 dB across the 50 kHz to 300 MHz band.

Repeatable connections were found to be a problem due to the mechanical stress placed on the fiber connectors. The data in Table 4 represents the optimized throughput of each configuration. This was achieved by flexing the transmitter and receiver connectors with respect to the fiber box until a maximum signal was achieved.

B. PULSE DELAY

The pulse delay time is governed by the length L of fiber and is given by

$$\tau = \frac{Ln}{c} \quad , \tag{1}$$

where n≈1.45 is the effective index of the fiber, and c = 3 x 10^8 m/sec is the velocity of light. For a 475±26 m fiber, the expected delay is 2.3±0.1 μsec. Figure 14 shows the delay time of the transmitter-fiber-receiver package for the three transmitters. The measured 2.2-μsec delay is in agreement with the 475±26 m length measured on the Hughes OTDR.

Table 4. Small-Signal Gain of the Transmitter-Fiber-Receiver Link

f, MHz	Tx 1 Gain, dB	Tx 2 Gain, dB	Tx 3 Gain, dB
0.01	-9.5	-6.0	-2.5
0.02	-3.5	0.8	3.6
0.03	-1.9	3.4	5.5
0.05	-1.2,-0.6	5.0	6.2
0.10	-0.7,-0.6	6.0	6.5
0.20	-0.6	6.0	6.5
0.33	-0.3	6.0	7.0
0.50	0	6.2	7.2
1.0	0	6.4	7.2
2.0	0.8	6.6	7.1
3.3	0.6	6.5	7.2
5.0	0.6	6.6	7.2
10	0.4,0.6	6.4	7.6
20	0.8	6.4	7.2
30	0.8	6.4	7.0
50	1.2	6.0	7.2
100	1.2	6.0	6.8
200	0.4	4.8	6.0
300	0.4±0.4	4.8	6.0
500	0.8±0.4	2.4	4.0

7037

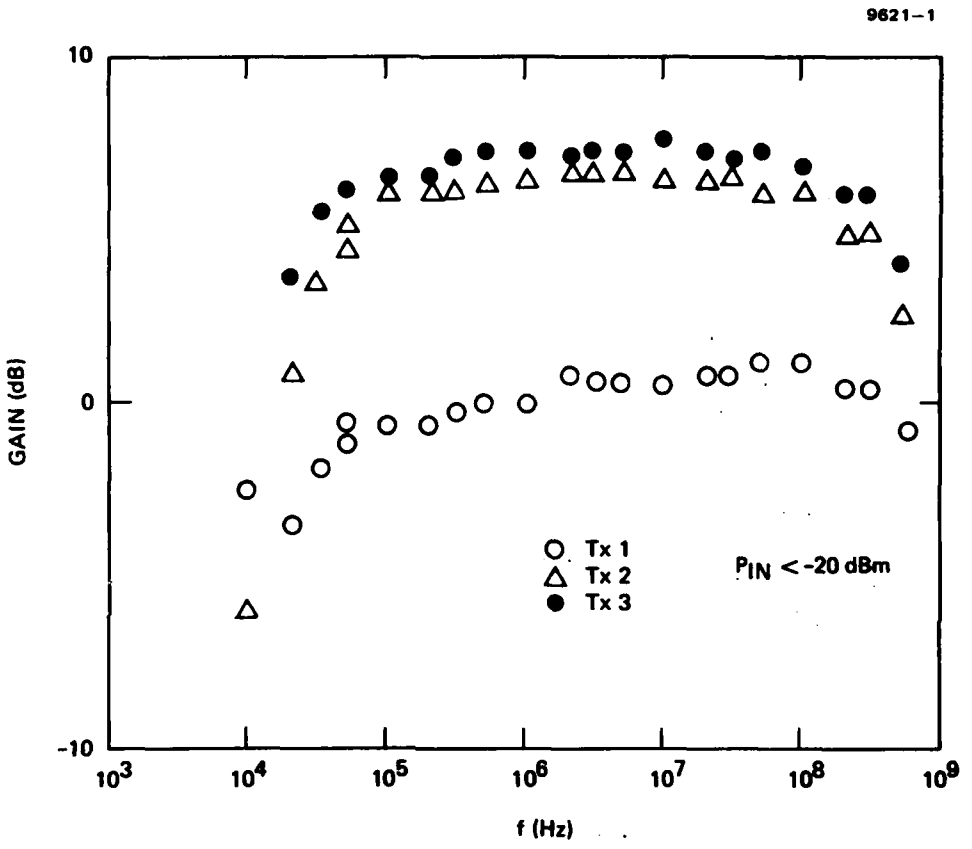

Figure 13. Insertion loss (or gain) as a function of frequency for the three transmitters coupled through the delay fiber to the receiver.

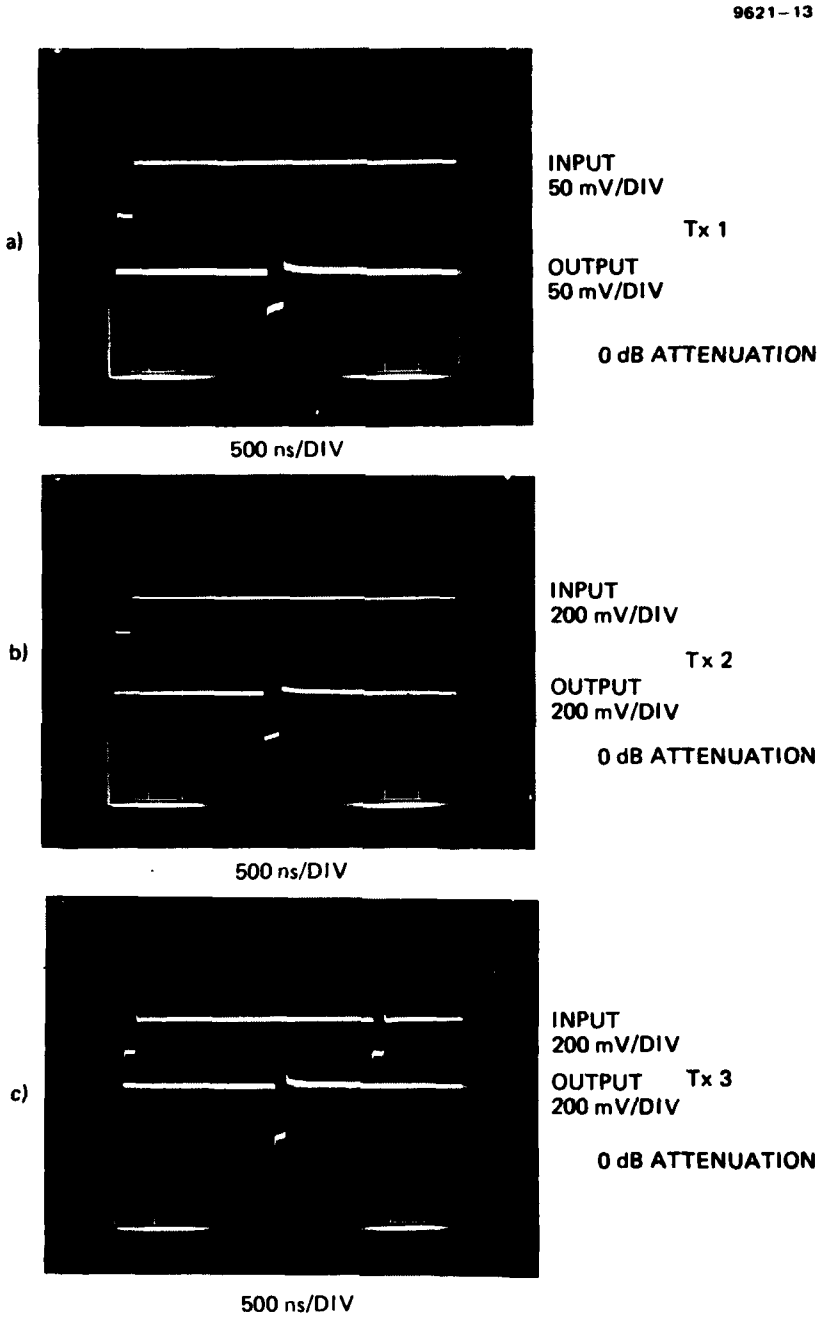

Figure 14. Delay times for the three transmitters.

C. SIGNAL DISTORTION

Signal distortion in the transmitter occurs because the optical power versus current (P-I) characteristics of the laser are nonlinear and because the laser rate equations are also nonlinear. Several types of distortion can occur: harmonic distortion or intermodulation products, amplitude distortion (e.g., gain compression), and phase distortion (e.g., AM to PM). Harmonic distortion and gain compression were characterized using sinusoidal signals. Pulse compression was also observed for positive and negative polarity signals.

1. Harmonic Distortion

The amount of second harmonic (2f) power relative to the fundamental (f) power at the output of the receiver is given in Figure 15. The rf input power into each of the transmitters is -10 dBm. The second harmonic power is below 25 dB of the fundamental power across the frequency range of interest for Tx 1 and below 30 dB for Tx 2 and Tx 3. The third harmonic (3f) power is shown in Figure 16. For Tx 1, the third harmonic power is more than 25 dB below the fundamental, and for Tx 2 and Tx 3, it is more than 35 dB below for a fundamental input power level of -10 dBm. The harmonic products could also be attributed to the photodiode or the receiver amplifiers. The intermodulation products generated by the amplifiers are below the levels shown in Figures 15 and 16. If the photodiode were at fault, then the harmonic distortion from Tx 1 should be less because it has a lower efficiency than Tx 2 and Tx 3. However, just the opposite is the case. Thus, it is reasonable to assume the lasers are responsible for the harmonic distortion.

2. Amplitude Distortion

The rf output power of the receiver versus the rf input power to each of the transmitters is shown in Figures 17 through 19 for 1 and 300 MHz. Tx 1, Tx 2, and Tx 3 deviate from linearity (1-dB gain compression) at input levels in excess of -5 dBm, 0 dBm, and -10 dBm, respectively. These values are far below the gain compression levels

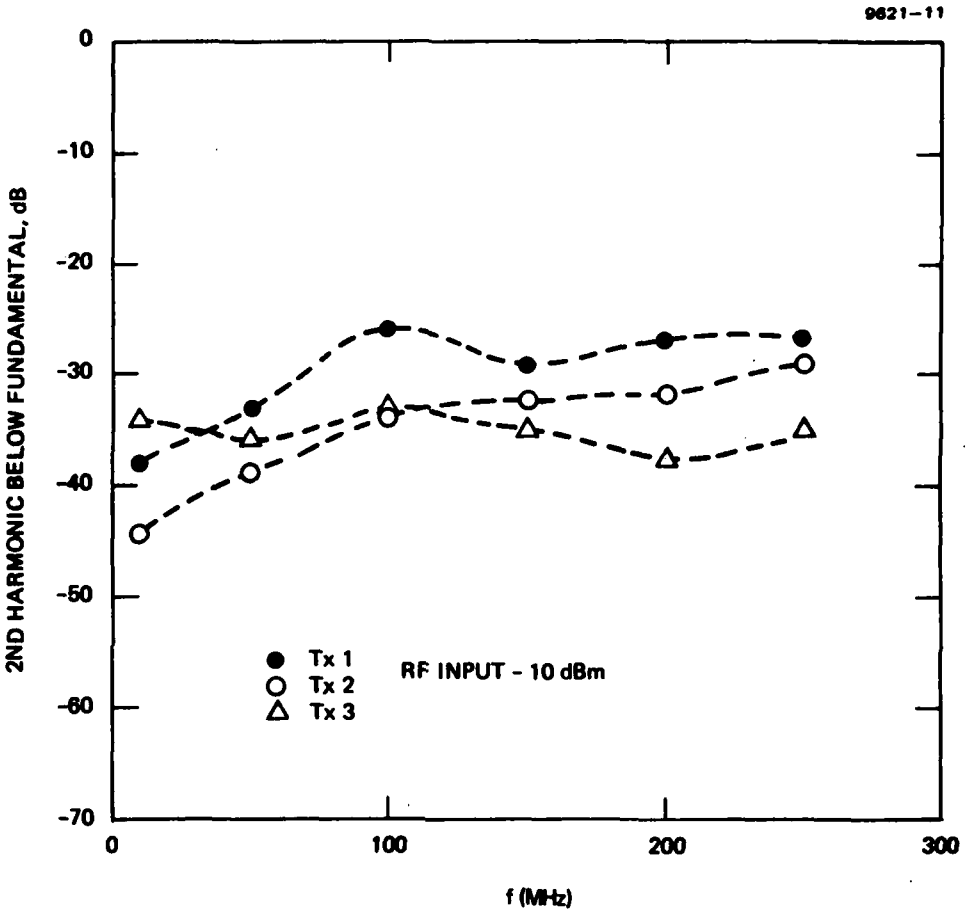

Figure 15. Second harmonic distortion products as a function of the fundamental frequency f.

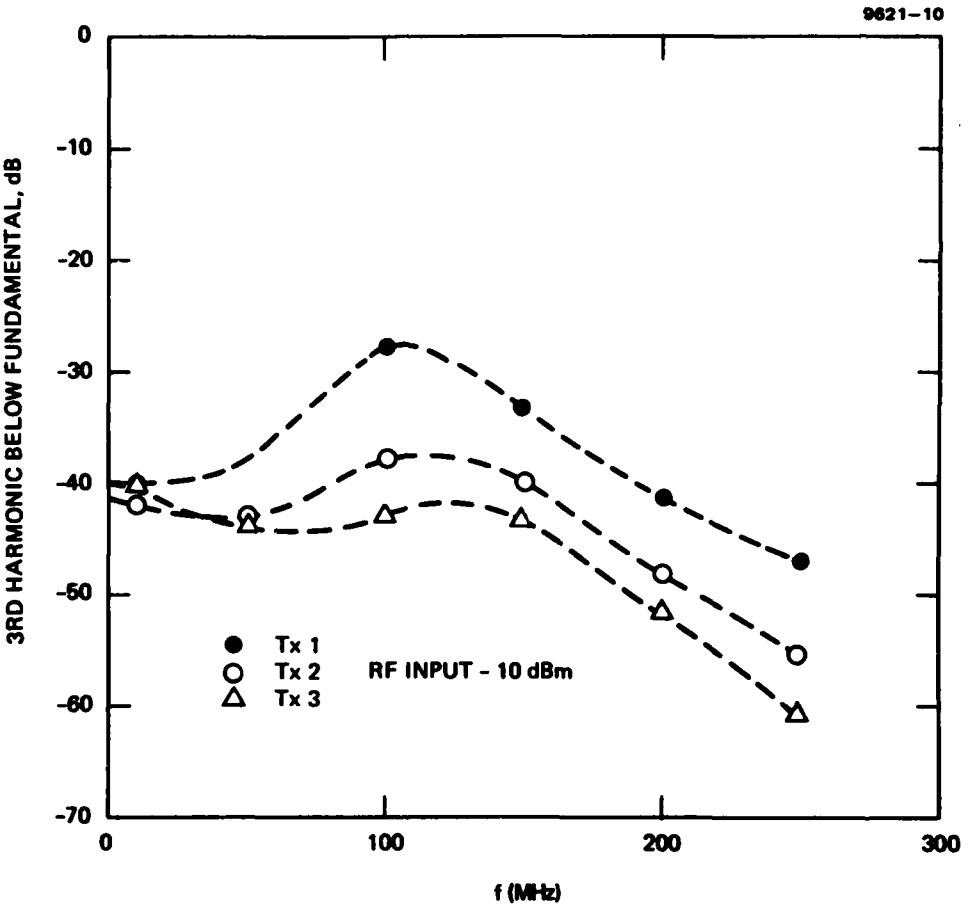

Figure 16. Third harmonic distortion products as a function of the fundamental frequency f.

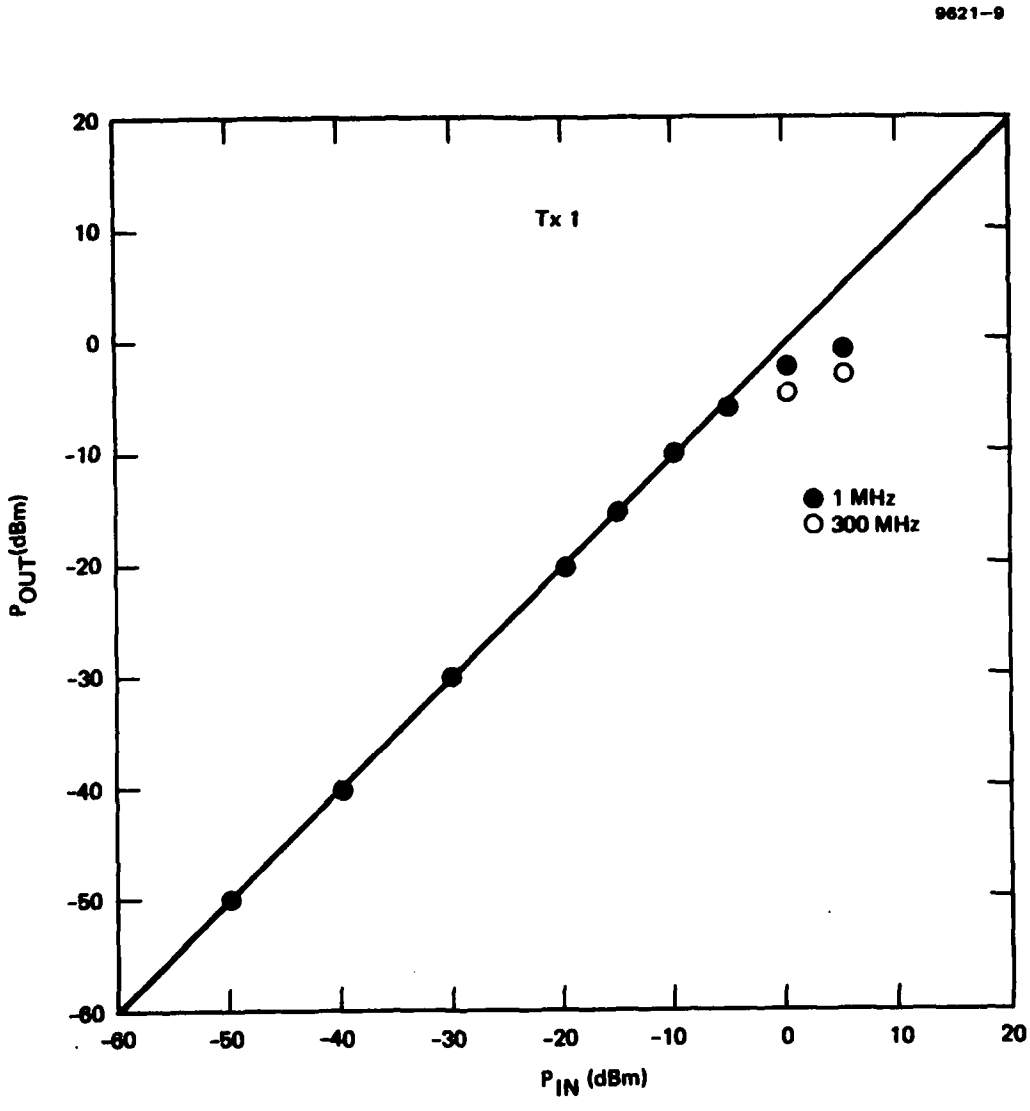

Figure 17. Amplitude distortion of Tx 1.

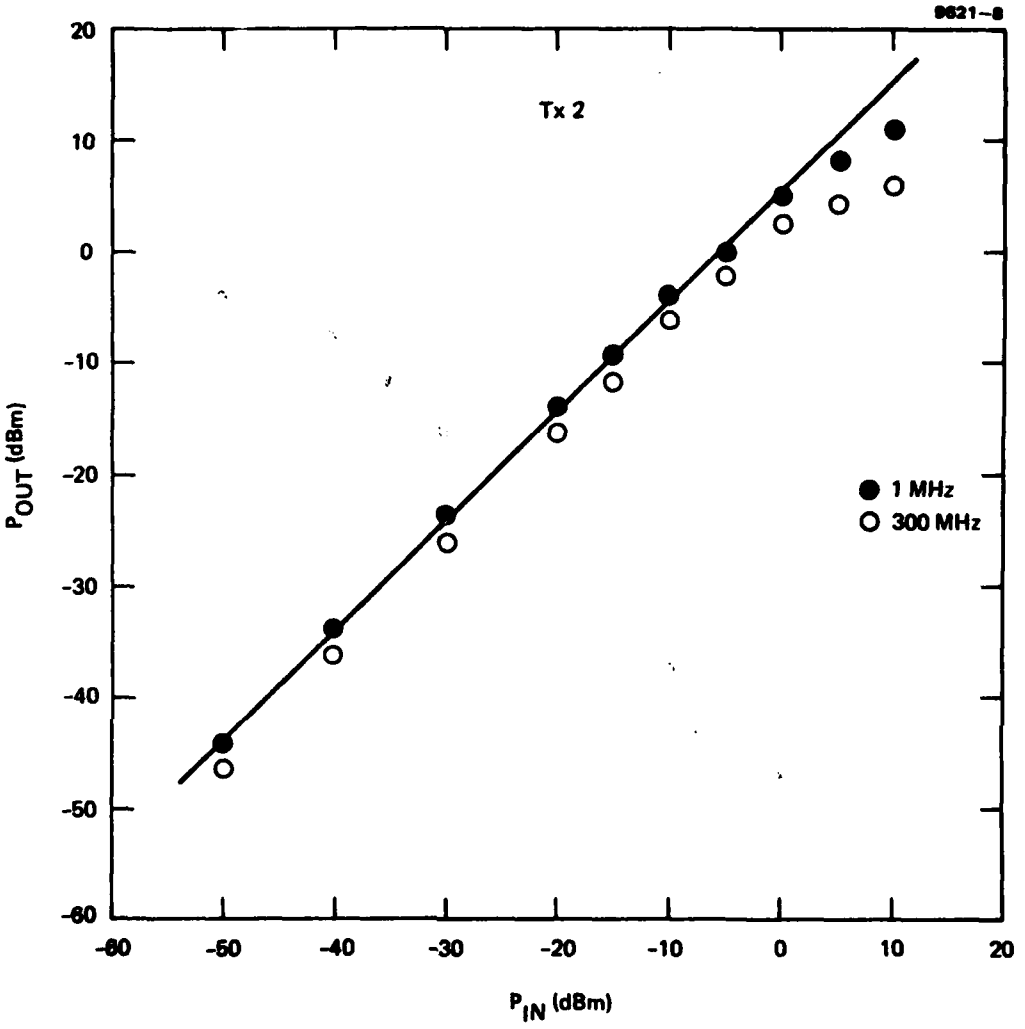

Figure 18. Amplitude distorion of Tx 2.

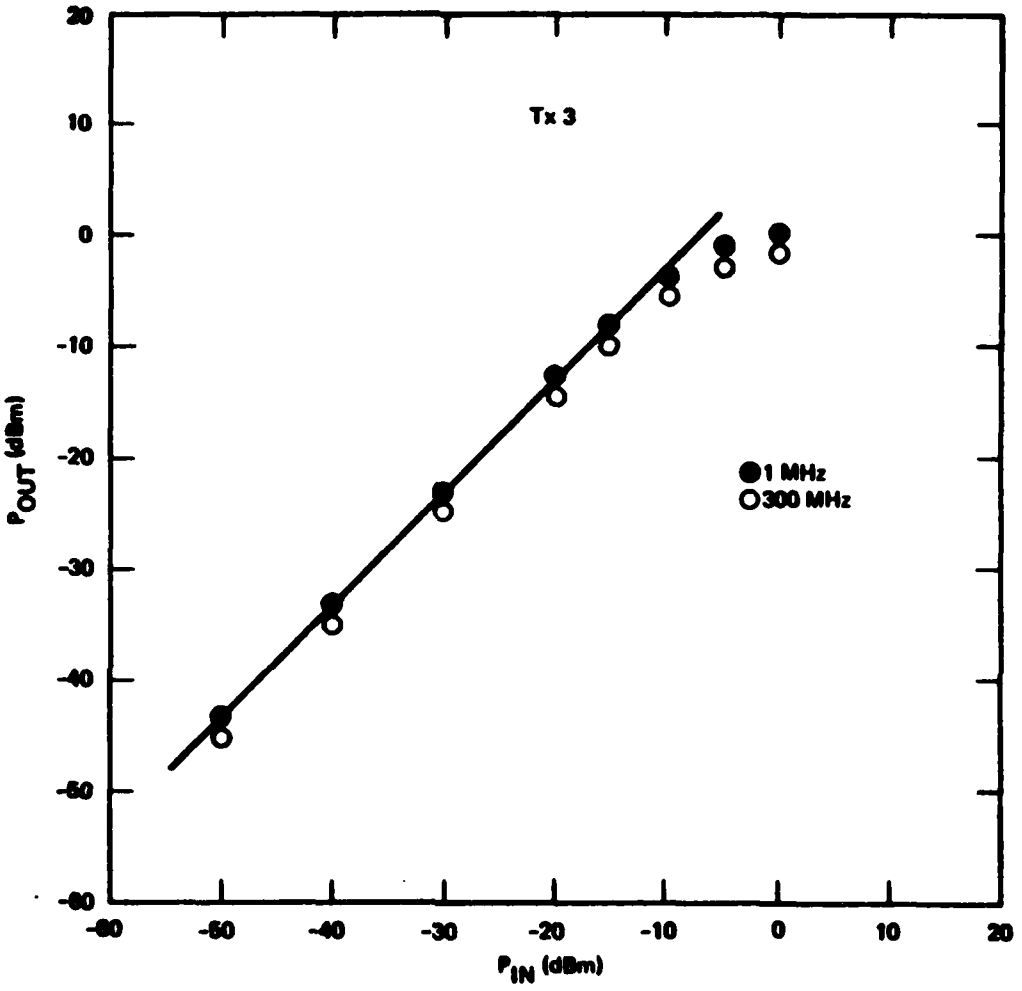

Figure 19. Amplitude distortion of Tx 3.

for the amplifiers. Since the photodiode does not start to saturate under cw conditions until 1 mW, it cannot be the cause of the 1 dB compression. A current of 6 mA (0 dBm into 50 Ω) would cause a power change of only 0.5 mW at the detector for a 20% external laser efficiency and a 4-dB fiber loss. The maximum cw level at the detector is 0.3 mW (from Tx 2), so an added 0.5 mW means the instantaneous optical power will be under 1 mW for an rf input of 0 dBm. Furthermore, Tx 2 has the greatest output power and yet also has the greatest compression point. This indicates that the cw operating point of Tx 2 is farther above threshold than is Tx 1 and that Tx 3 is nearest threshold.

Figures 20 through 22 give oscilloscope traces of the response of the transmitter-fiber-receiver system to sinusoidal signals at 200 kHz and 50 MHz for Tx 1, Tx 2, Tx 3, respectively. Distortion of the signal in Tx 3 is apparent in Figure 22(e) from the clipping of the upper portion of the sine wave. This corresponds to driving the laser near threshold.

3. Pulse Response

Figure 23 shows the P-I characteristic of the laser. From the sign convention in Figure 5, a positive polarity pulse tends to drive the laser closer to threshold and a negative polarity pulse to drive the laser farther above threshold. Figure 24 is the response of the Tx 1-fiber-receiver combination to a 50-nsec pulse of varying amplitude (input attenuation) and polarity. As expected, the negative pulse in Figure 24(c) does not suffer compression compared to its positive counterpart. Figure 25 is the pulse response of Tx 2, and Figure 26 is for Tx 3.

D. SYSTEM NOISE AND DYNAMIC RANGE

There are several noise sources that can degrade the dynamic range of the delay line: laser noise, receiver shot noise, and receiver amplifier noise. For ideal shot noise, the shot noise power at the input of the preamp is

$$P_s = 2qI_D R_L B \quad , \tag{2}$$

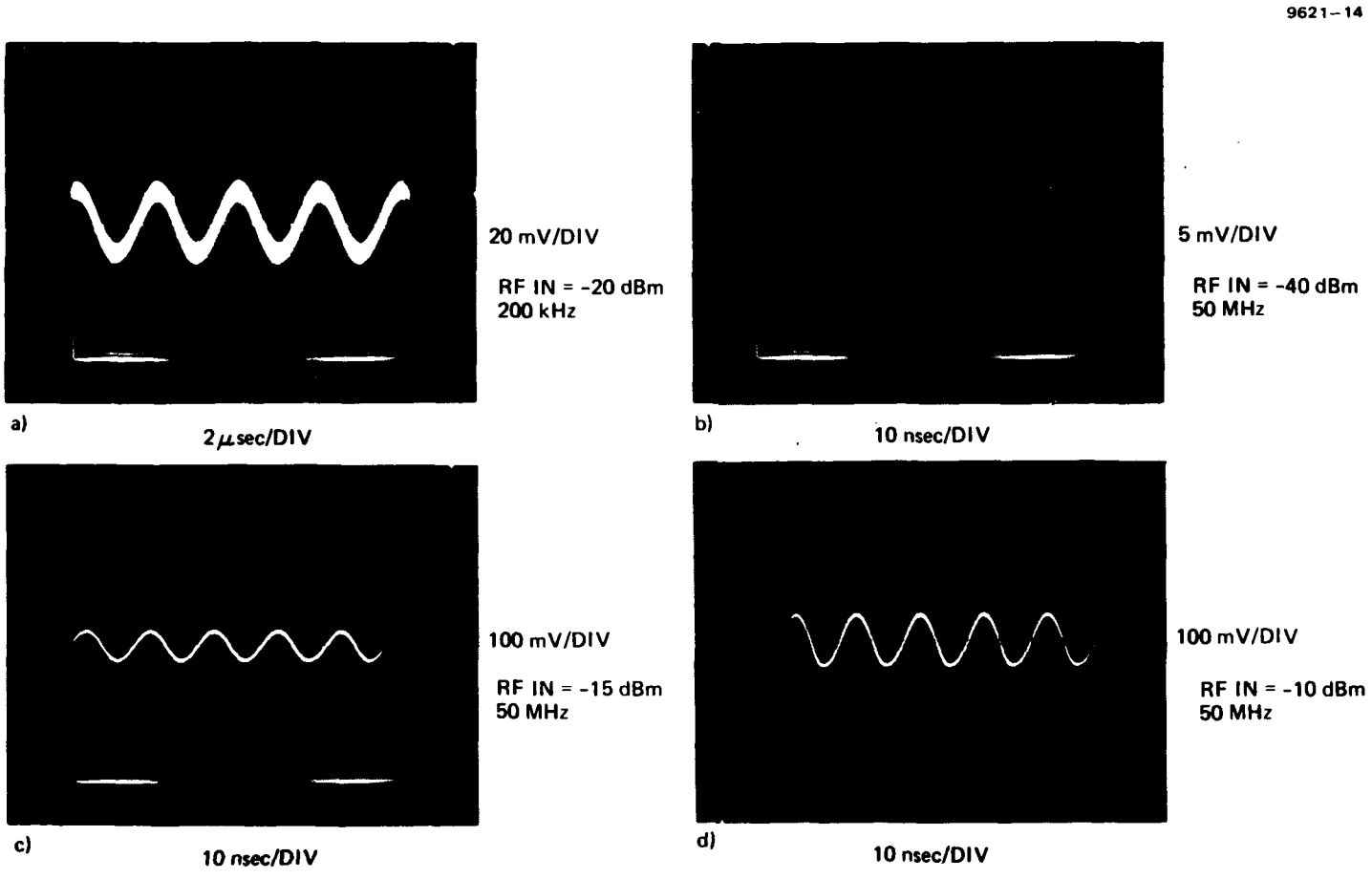

Figure 20. Response of the Tx 1-fiber-receiver combination to (a) -20 dBm 200 kHz input, (b) -40 dBm 50 MHz input, (c) -15 dBm 50 MHz input, and (d) -10 dBm 50 MHz input.

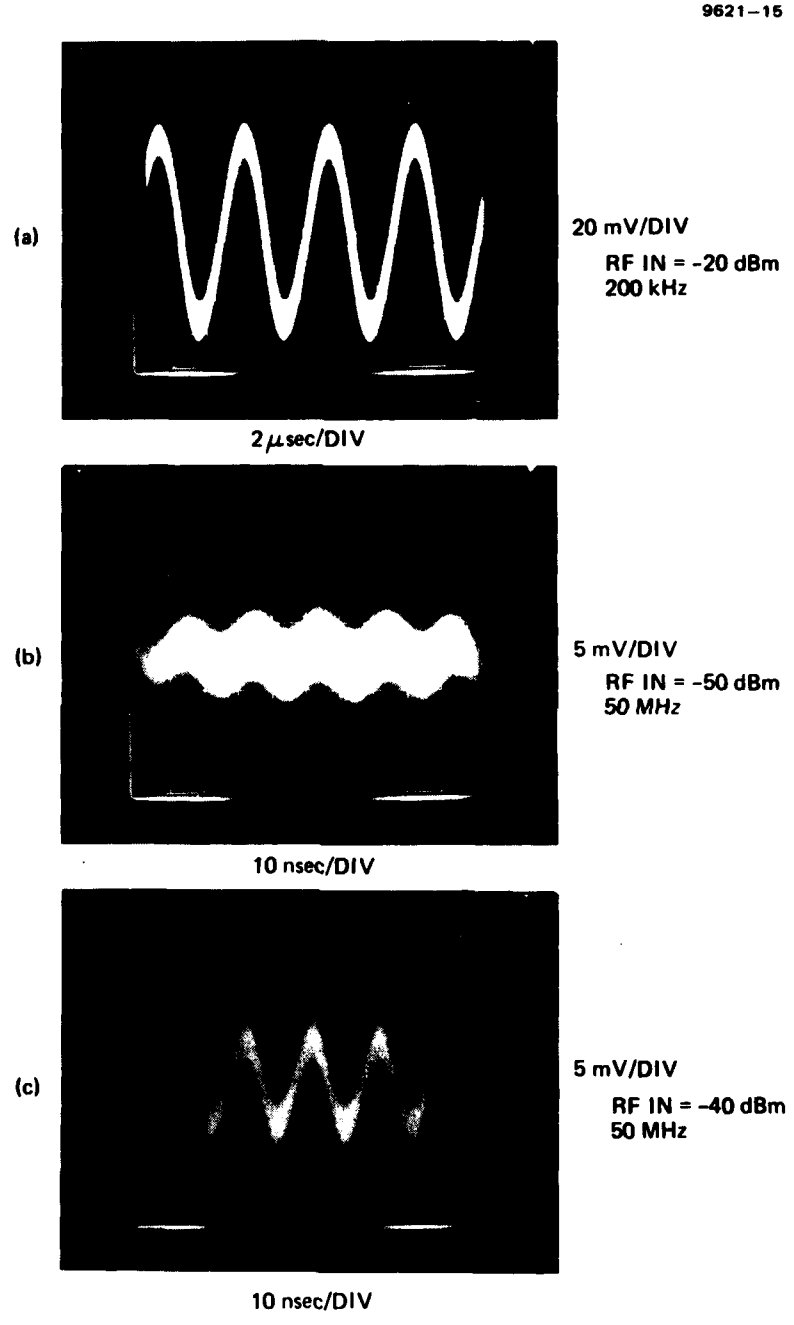

Figure 21. Response of the Tx 2-fiber-receiver combination to (a) -20 dBm 200 kHz input, (b) -50 dBm 50 MHz input, (c) -40 dBm 50 MHz input, (d) -15 dBm 50 MHz input, and (e) -10 dBm 50 MHz input.

9621-16

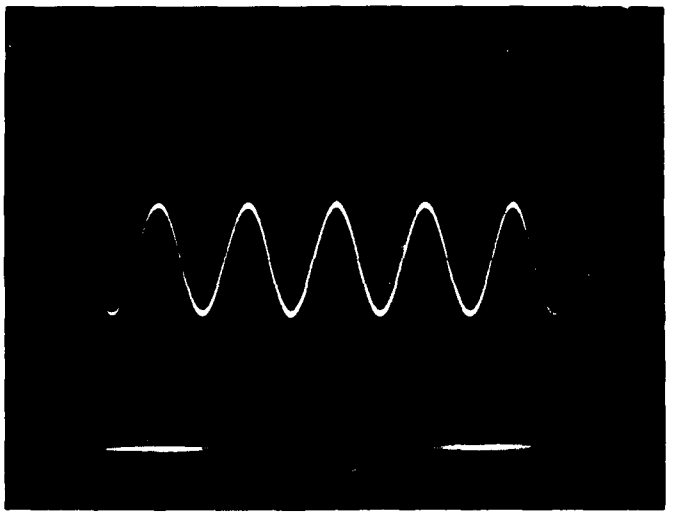

(d)

100 mV/DIV
RF IN = -15 dBm
50 MHz

10 nsec/DIV

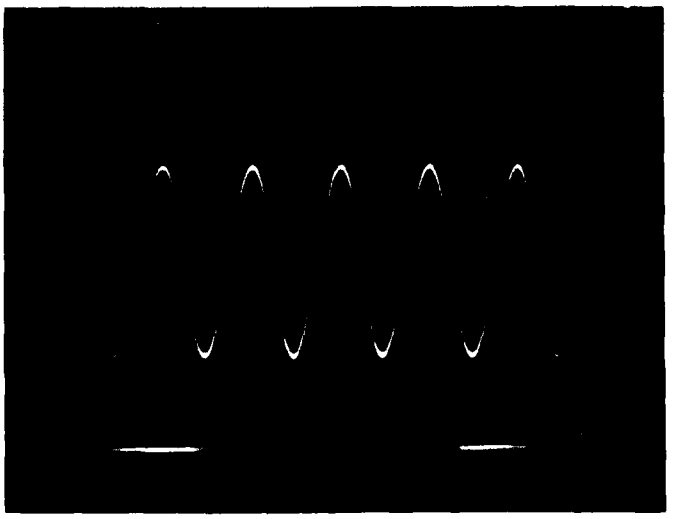

(e)

100 mV/DIV
RF IN = -10 dBm
50 MHz

10 nsec/DIV

Figure 21. Continued.

9621-17

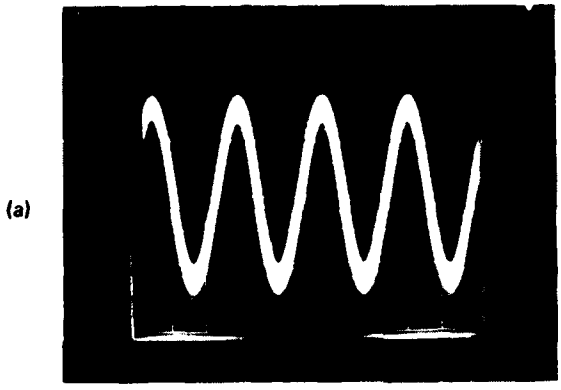

(a)

20 mV/DIV

RF IN = -20 dBm
200 kHz

2μsec/DIV

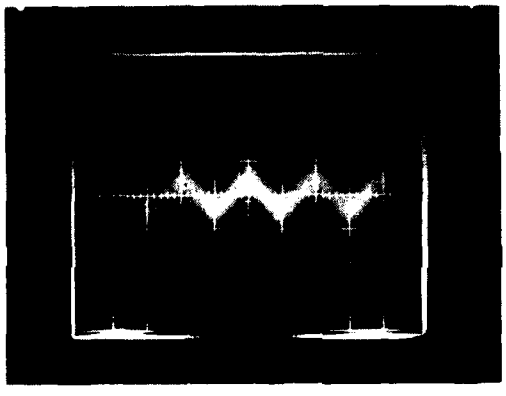

(b)

5mV/DIV

RF IN = -50 dBm
50 MHz

10 nsec/DIV

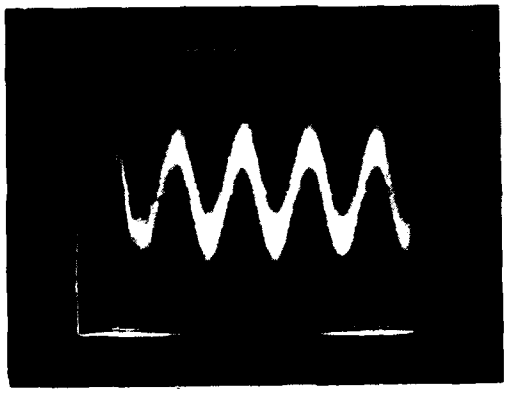

(c)

5 mV/DIV

RF IN = -40 dBm
50 MHz

10 nsec/DIV

Figure 22. Response of the Tx 3-fiber-receiver combination to (a) -20 dBm 200 kHz input, (b) -50 dBm 50 MHz input (c) -40 dBm 50 MHz input, (d) -15 dBm 50 MHz input, and (e) -10 dBm 50 MHz input.

9621-18

(d)

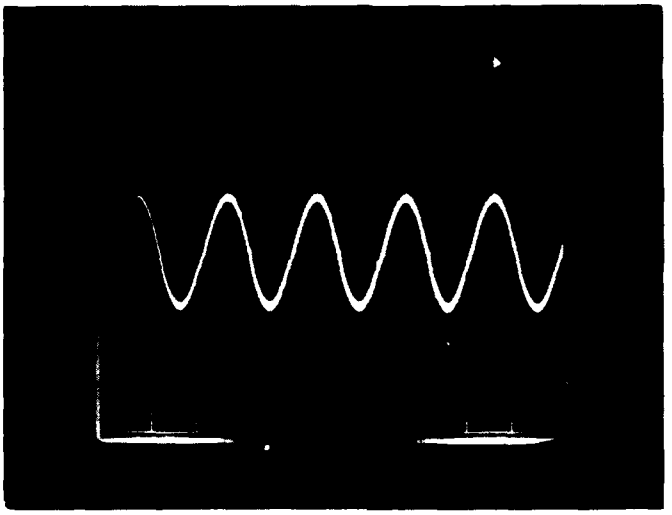

100 mV/DIV
RF IN = -15 dBm
50 MHz

10 nsec/DIV

(e)

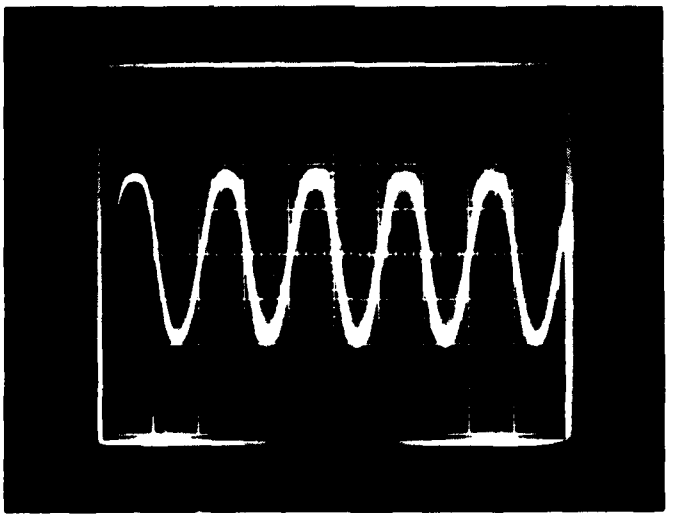

100 mV/DIV
RF IN = -10 dBm
50 MHz

10 nsec/DIV

Figure 22. Continued.

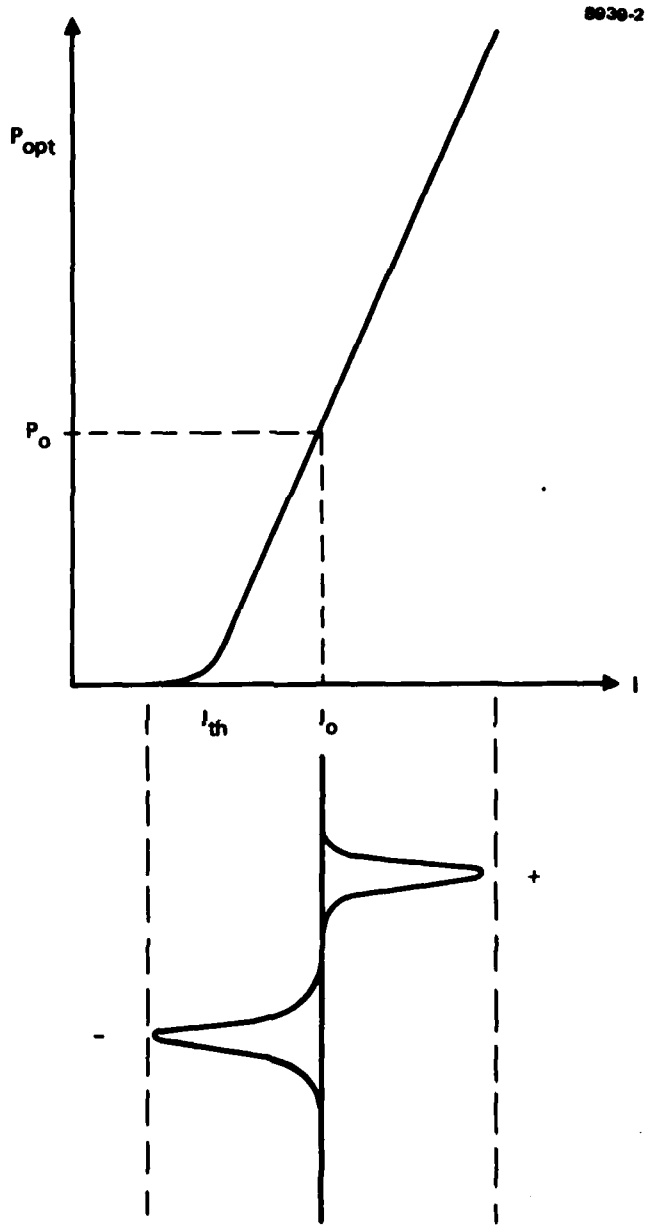

Figure 23. Laser output power versus current.

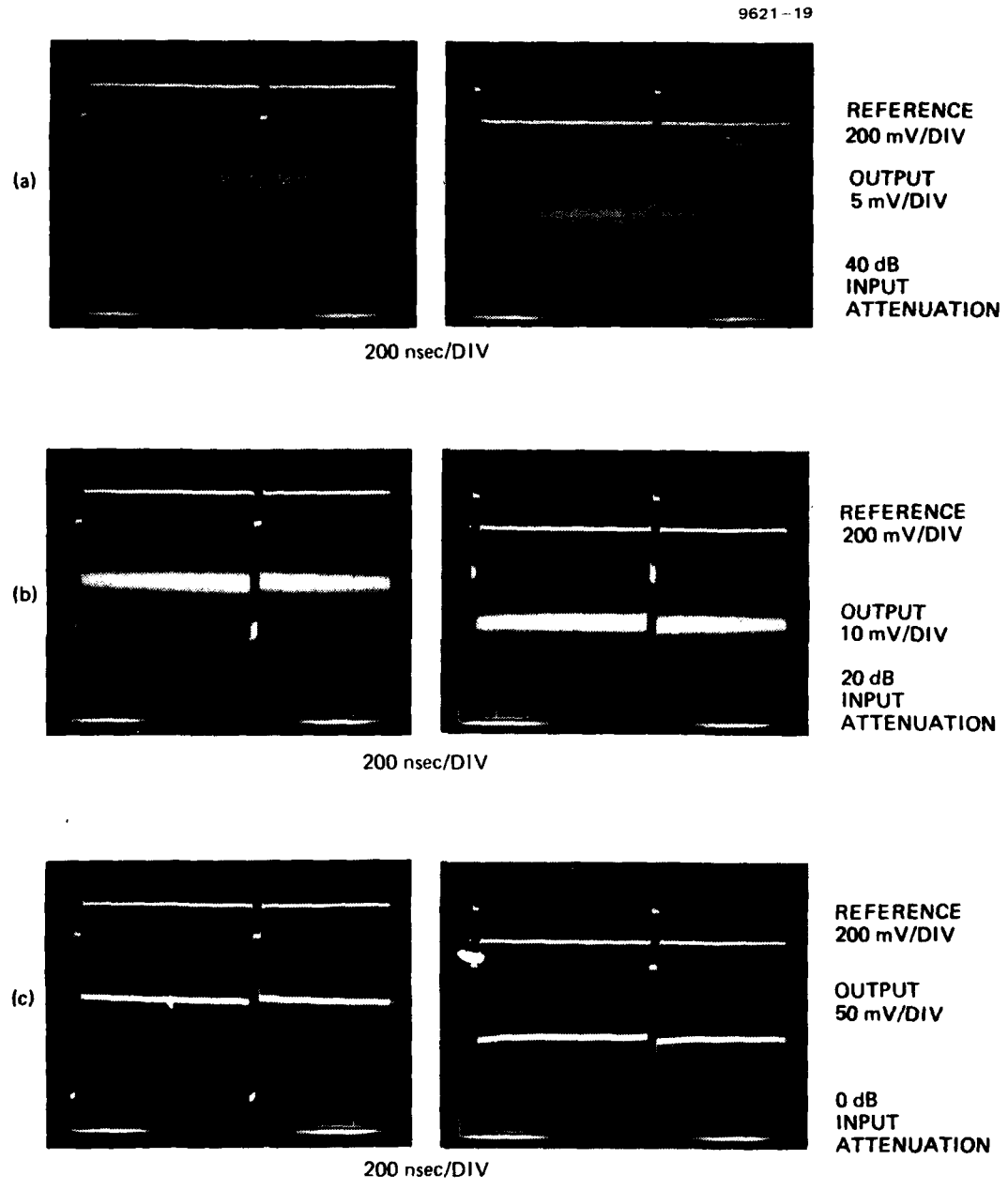

Figure 24. Pulse response of the Tx 1-fiber-receiver combination.

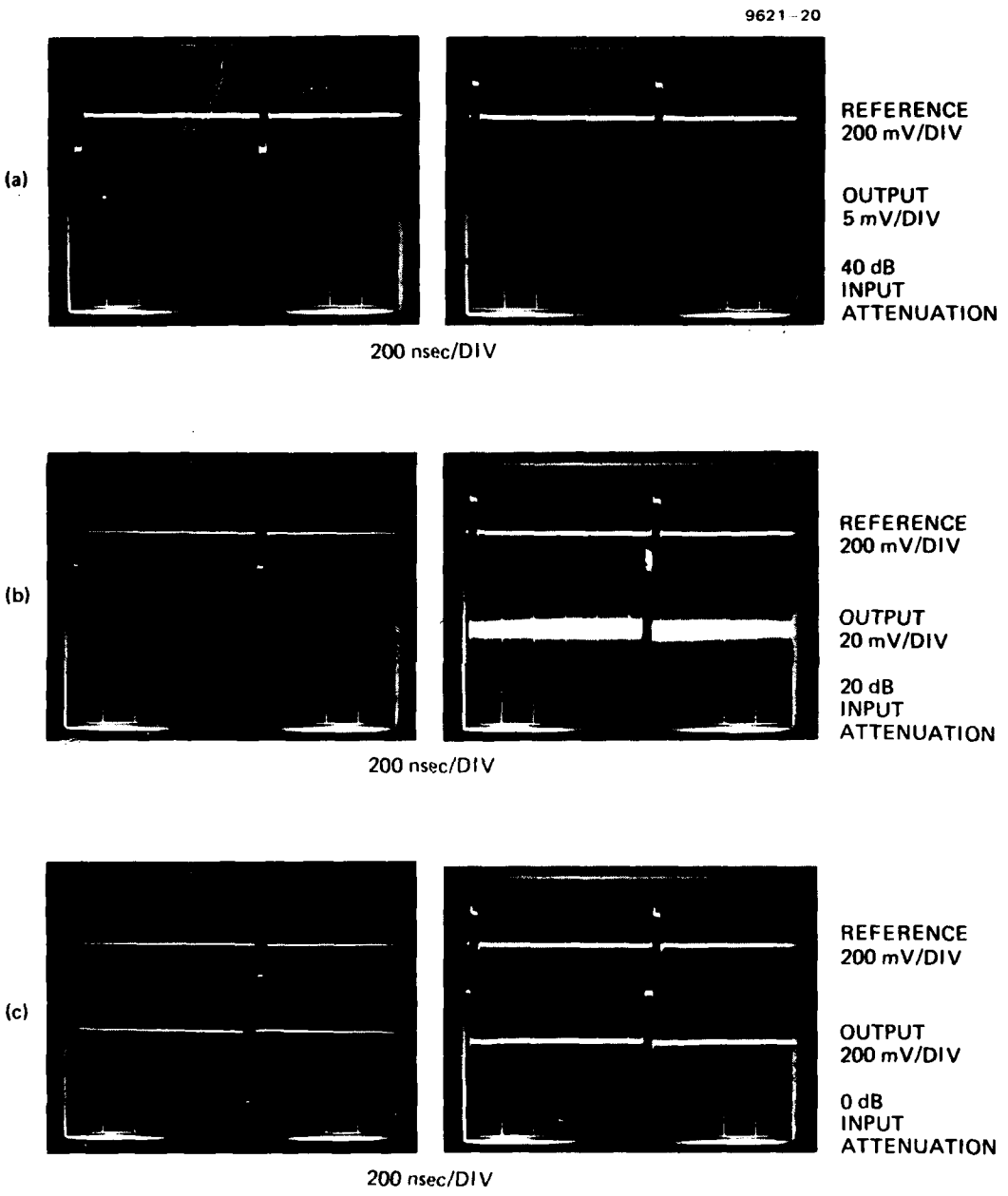

Figure 25. Pulse response of the Tx 2-fiber-receiver combination.

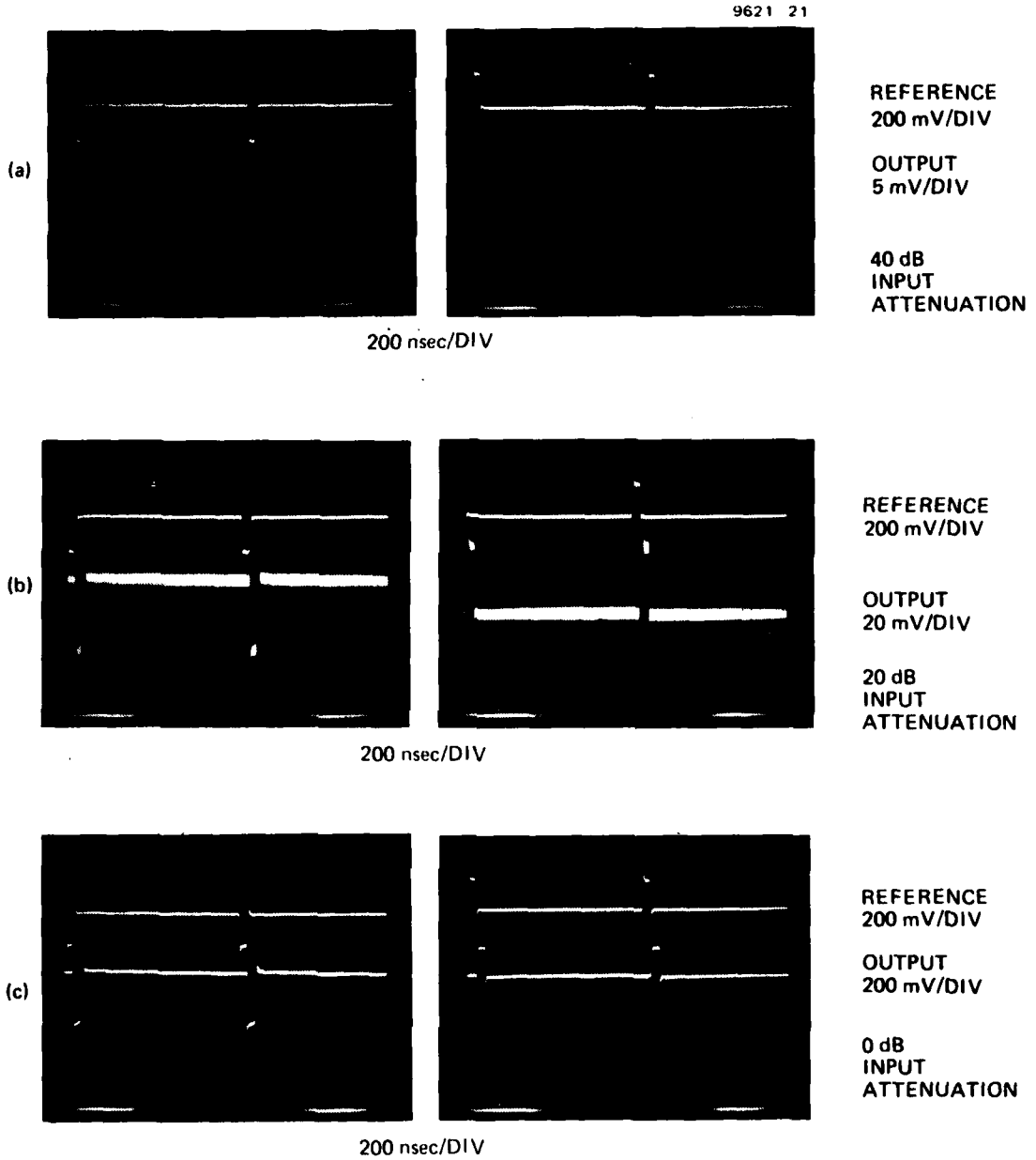

Figure 26. Pulse response of the Tx 3-fiber-receiver combination.

where I_D is the cw detector current, R_L is the preamp input resistance, and B is the bandwidth. The amplifier noise power at its input is

$$P_a = kT_o(F_a-1)B \quad , \tag{3}$$

where k is Boltzmann's constant, $T_o = 290^oK$, and F_a is the amplifier noise figure. If $F_a \simeq 7.5$ dB for the GPD-463, a detector current in excess of 1 mA (or 5 mW optical power incident on the 5082-4207 pigtail) would be required for the shot noise to equal the amplifier noise. Thus, shot noise can be neglected in this system.

Figure 27 is the noise out of the receiver without any cw transmitter input. The total noise output power from the load resistor and amplifier is

$$P_o = kT_oF_aG_aB \quad , \tag{4}$$

where G_a is the amplifier gain. If the GPD-463 has a gain of 10 dB and a noise figure of 7.5 dB, and the AV-1M has a gain of 30 dB and a noise figure of 9 dB, the total amplifier gain is 40 dB and the total noise figure is 8 dB. The theoretical noise power output (Eq. 4) over a 500-MHz bandwidth is -39 dBm. The noise power in Figure 27 is ≃-38 dBm.

A second technique that gives a more accurate measure of the receiver noise power is shown in Figure 28. An HP 8447D preamp and HP 432A/8478B power meter are used. The combined frequency response of the preamp/power meter is flat above 3 MHz. However, the response is 3 dB down at 1 MHz and 14 dB down at 100 kHz. Therefore, this technique only measures the noise from 1 MHz and up. (The low-frequency cut-off of the 8565A is 10 MHz). The noise power output measured by this technique without cw transmitter power was -38 dBm, in agreement with the spectrum analyzer technique.

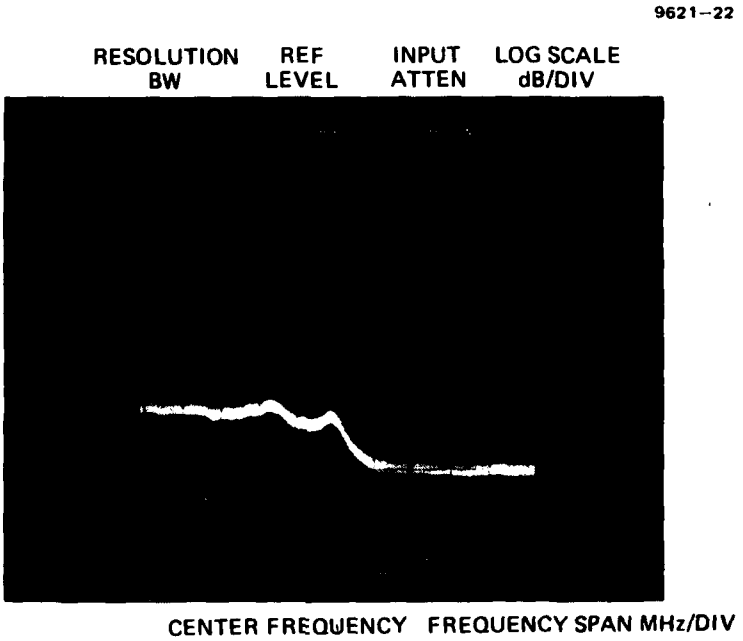

Figure 27.
Receiver noise output without transmitter input measured on an HP 8565A spectrum analyzer. The noise power is -67 dBm/MHz +1.7 dB spectrum analyzer correction factor for log amplifier and filter response. Over a 500 MHz bandwidth, the total noise power output is -38 dBm.

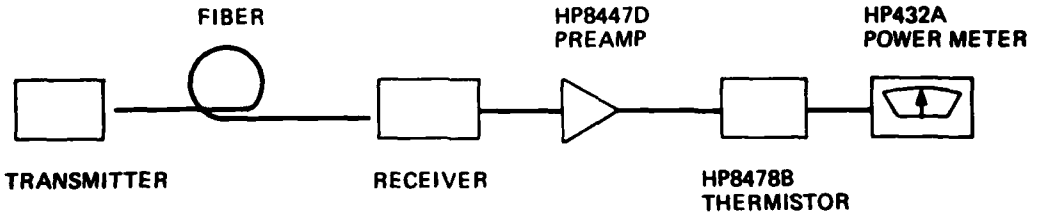

Figure 28. Noise power measurement technique. The HP8447D contributed an insignificant amount to the total noise.

The total transmitter-fiber link-receiver noise was measured by running each of the transmitters cw (no rf input). Figure 29 shows the results of these measurements on the spectrum analyzer. Noise resonances at multiples of the frequency

$$f_n = \frac{c}{2n\ell} \simeq \frac{3 \times 10^8 \text{ m/sec}}{2 \times 1.45 \times 0.06 \text{ m}} \simeq 170 \text{ MHz} \qquad (5)$$

are due to reflection feedback at the laser pigtail-fiber connector, where $\ell \simeq 60$ cm is the laser pigtail length. If the connector is filled with an index-matching fluid such as glycerin, the reflection at the connector will be reduced and the noise resonances due to the feedback into the laser will be diminished. The difference in the receiver noise characteristcs with and without glycerin in the laser-fiber connector can be seen in Figure 29. The noise output of each transmitter-fiber-receiver combination was measured using the technique shown in Figure 28, and the results are presented in Table 5 along with the delay line gain, bandwidth, and compression level.

The noise power out of the receiver was greater with the transmitters on. This was not expected from the shot-noise calculations. It is not known what the fluctuations (up to ±3 dBm) in the noise power of the transmitters are due to. With glycerin in the laser-fiber connector, the noise decreased for Tx 1 and Tx 2 while it increased for Tx 3. However, the change in average noise in all cases was within the value of fluctuations observed. Therefore, no quantitative conclusions can be drawn about the source of excess laser noise or the effect of using an index-matching fluid. Furthermore, an index-matching fluid should not be used in the Hughes fiber connectors as it will collect dust and foreign material over a period of time.

The equivalent noise power at the input of each transmitter is calculated by subtracting the transmitter-fiber-receiver gain from the noise output power. The system dynamic range on Table 5 is the difference of the 1-dB compression input power and the equivalent input noise

9621-23

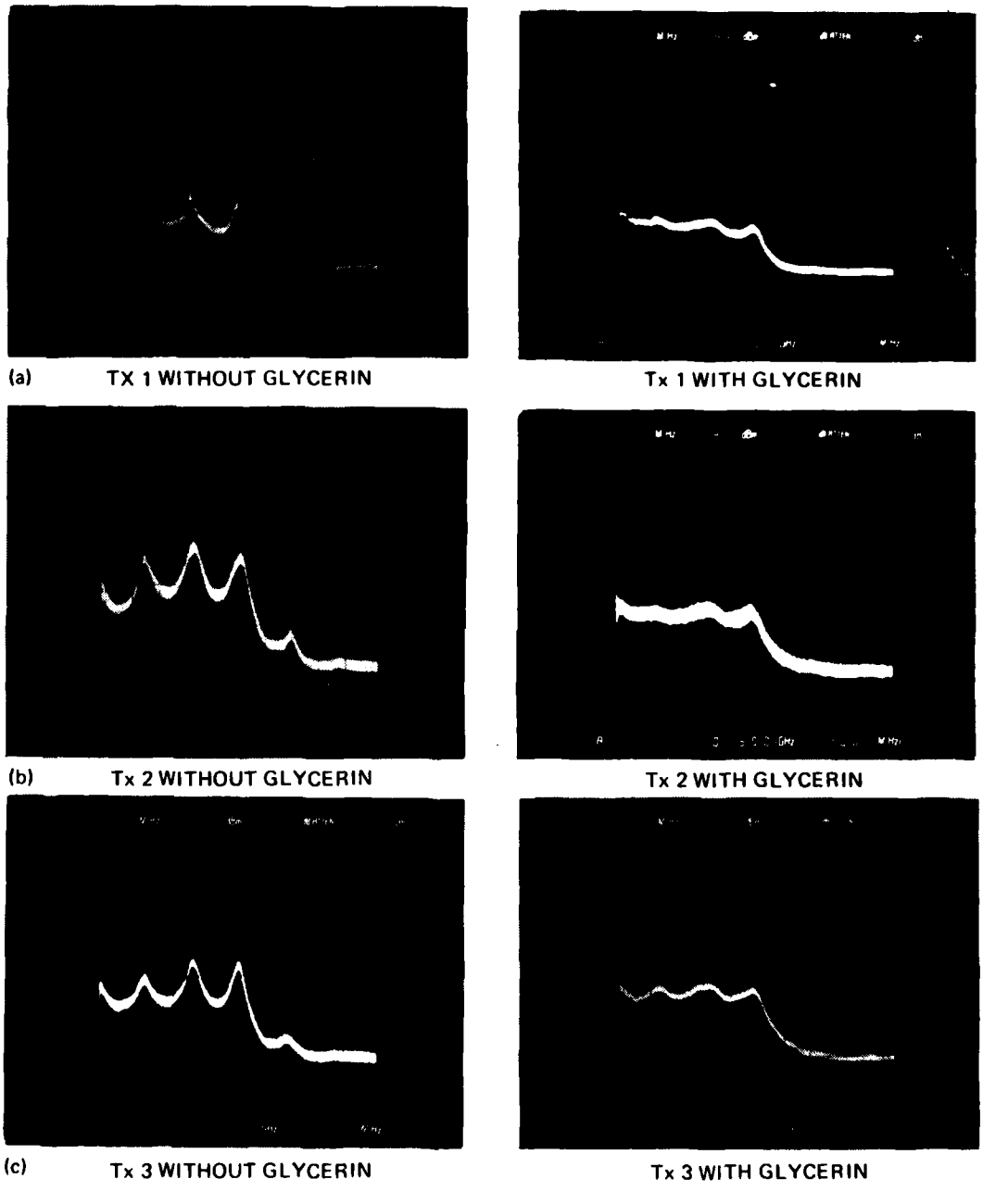

Figure 29. System noise with the various transmitters.

Table 5. Summary of Transmitter-Fiber-Receiver Characteristics

Quantity	Tx 1	Tx 2	Tx 3
Small-signal gain (±1 dB), dB	0	5.6	6.6
±1 dB bandwidth	50 kHz to 500 MHz	50 kHz to 300 MHz	30 kHz to 300 MHz
1 dB input compression power, dBm	>-5	>0	>-10
Noise output of receiver (w/o glycerin), dBm	-35±3	-30±3	-32±2
Equivalent noise at input of transmitter (w/o glycerin), dBm	-35±3	-36±3	-39±2
Noise output of receiver (with glycerin), dBm	-37±3	-34±1	-30±2
Equivalent noise at input of transmitter (with glycerin), dBm	-37±3	-40±1	-37±2
Dynamic Range, dBm	30±3	36±3	29±2
The ±2 and ±3 dBm represent the noise power fluctuation			

power. (This lower limit is a S/N ratio of 1.) All three transmitter-fiber-receiver configurations have a nominal dynamic range of 30 dB. It is interesting to note that the transmitter with the largest dynamic range (Tx 2) is also the one that is driven farthest above threshold.

SECTION 4

CONCLUSIONS

All of the performance specifications were met for this contract. However, several problem areas were identified for improvement on future fiber-optic links.

The repeatability of the throughput efficiency needs to be improved by allowing flexible cable connections between the laser pigtail and fiber and between the receiver and fiber (as opposed to fixing the connectors to the various chassis). Furthermore, laser feedback noise is a critical issue. Several possible solutions exist: (1) use of an optical isolator; (2) reduction of the pigtail connector reflection by use of index matching fluid, etc.; or (3) elimination of the first connector by use of a fiber splice.

Even with the use of an index-matching fluid, all three transmitters displayed noise that was in excess of the receiver by several dB. The source of this noise must be understood and reduced to increase the dynamic range. Also, the large fluctuations (±3 dB) of the receiver noise output must also be isolated in future work.

Table 6 summarizes the contract goals and the results achieved.

Table 6. Summary of Contract Goals and Results Obtained

Quantity	Goals	Tx 1	Tx 2	Tx 3
Bandwidth	<250 kHz to 250 MHz	50 kHz to 500 MHz	50 kHz to 300 MHz	30 kHz to 300 MHz
Throughput efficiency	Flat to ±1 dB	-1 to +1 dB	4.6 to 6.6 dB	5.6 to 6.6 dB
Linearity	1 dB compression as maximum input power	>-5 dBm	>0 dBm	>-10 dBm
Transmitter stability	±0.1%	better than ±0.3%	better than ±0.7%	better than ±0.3%
Dynamic range	≥30 dB	>30±3 dB	>36±3 dB	>29±3 dB
Delay	2.4 μsec	2.2 μsec	2.2 μsec	2.2 μsec

7037